NUMERICAL MODELING OF WIND WAVE INDUCED LONGSHORE SEDIMENT TRANSPORT

A THESIS SUBMITTED TO
THE GRADUATE SCHOOL OF NATURAL AND APPLIED SCIENCES
OF
MIDDLE EAST TECHNICAL UNIVERSITY

BY

ILGAR ŞAFAK

IN PARTIAL FULFILLMENT OF THE REQUIREMENTS
FOR
THE DEGREE OF MASTER OF SCIENCE
IN
CIVIL ENGINEERING

JULY 2006

Approval of the Graduate School of Natural and Applied Sciences

_____
Prof.Dr. Canan Özgen
Director

I certify that this thesis satisfies all the requirements as a thesis for the degree of Master of Science.

_____
Prof.Dr. Erdal Çokça
Head of Department

This is to certify that we have read this thesis and that in our opinion it is fully adequate, in scope and quality, as a thesis for the degree of Master of Science.

_____
Dr.Işıkhan Güler
Co-Supervisor

_____
Prof.Dr. Ayşen Ergin
Supervisor

Examining Committee Members:

Prof.Dr. Halil Önder	(METU, CE)	_____
Prof.Dr. Ayşen Ergin	(METU, CE)	_____
Assoc.Prof.Dr. Ahmet Cevdet Yalçıner	(METU, CE)	_____
Dr. Işıkhan Güler	(METU, CE)	_____
Assoc.Prof.Dr. Mehmet Ali Kökpınar (DSİ (State Hydraulic Works))		_____

I hereby declare that all information in this document has been obtained and presented in accordance with academic rules and ethical conduct. I also declare that, as required by these rules and conduct, I have fully cited and referenced all material and results that are not original to this work.

Name, Last Name: Ilgar , ŞAFAK

Signature:

ABSTRACT

NUMERICAL MODELING OF
WIND WAVE INDUCED LONGSHORE SEDIMENT TRANSPORT

ŞAFAK, Ilgar

M.S., Department of Civil Engineering

Supervisor: Prof.Dr. Ayşen Ergin

Co-Supervisor: Dr. Işıkhan Güler

July 2006, 88 Pages

In this study, a numerical model is developed to determine shoreline changes due to wind wave induced longshore sediment transport, by solving *sediment continuity equation* and taking *one line theory* as a base, in existence of seawalls, groins, T-groins, offshore breakwaters and beach nourishment projects, whose dimensions and locations may be given arbitrarily. The model computes the transformation of deep water wave characteristics up to the surf zone and eventually gives the result of shoreline changes with user-friendly visual outputs. A method of representative wave input as annual average wave characteristics is presented. Compatibility of the currently developed tool is tested by a case study and it is shown that the results, obtained from the model, are in good agreement qualitatively with field measurements. In the scope of this study, input manner of long term annual wave data into model in miscellaneous ways is also discussed.

Keywords: Longshore sediment transport, Shoreline change, One-Line theory, Numerical modeling, Wave hindcasting

ÖZ

RÜZGAR DALGALARI SONUCU OLUŞAN KIYI BOYU KATI MADDE TAŞINIMININ SAYISAL MODELLEMESİ

ŞAFAK, Ilgar

Yüksek Lisans, İnşaat Mühendisliği Bölümü

Tez Yöneticisi: Prof.Dr. Ayşen Ergin

Ortak Tez Yöneticisi: Dr. Işıkhan Güler

Temmuz 2006, 88 Sayfa

Bu çalışmada, boyut ve yerleri rasgele verilebilen kıyı duvarları, mahmuzlar, T-mahmuzlar, açık deniz dalgakıranları ve kumsal beslemeleri varlığında, rüzgar dalgaları sonucu oluşan kıyı boyu katı madde taşınımının neden olduğu kıyı çizgisi değişimlerini *katı madde süreklilik denklemini* çözerek ve *tek çizgi teorisini* esas alarak belirleyen bir sayısal model geliştirilmiştir. Model, derin deniz dalga özelliklerini dalga kırılma bölgesine kadar taşımakta ve sonuçta kıyı çizgisinde meydana gelen değişimleri, görsel olarak kullanışlı çıktılar halinde vermektedir. Yıllık ortalama dalga özelliklerinin verilişinde, temsili dalga girdisi metodu sunulmuştur. Geliştirilen modelin tutarlılığı, uygulamalı bir çalışmayla test edilmiş ve modelden elde edilen sonuçların saha ölçümleriyle nitel olarak uyum içinde olduğu görülmüştür. Bu çalışma kapsamında, uzun dönem yıllık dalga verilerinin modele çeşitli şekillerde girilmesi de tartışılmıştır.

Anahtar Kelimeler: Kıyıboyu katı madde taşınımı, Kıyı çizgisi değişimi, Tek çizgi teorisi , Sayısal modelleme, Dalga tahmini

Dedicated to Cihat ŞAFAK and Şükran ŞAFAK

ACKNOWLEDGMENTS

I would like to thank Prof.Dr. Ayşen Ergin, Assoc.Prof.Dr. Ahmet Cevdet Yalçıner and Dr. Işıkhan Güler not only for their supervision throughout this study but also that they have trained me in coastal engineering profession. Besides, I am extremely grateful to them for including me into *Coastal Engineering Laboratory family* and mainly for those they kindly teach about life, which are much more valuable than all the coursework.

I dedicate my thanks to contributors of all referred studies and appreciate their resolution since they do not give up, in spite of several difficulties of faculty life.

Dr. Mehmet Ali Kökpınar and Dr.Yakup Darama, from General Directorate of State Hydraulic Works (DSI), are greatly acknowledged since they have strived to provide as much data and support as possible.

I give thanks to my dear friends Mr.Salih Serkan Artagan and Mr.Cüneyt Baykal, who have assisted me at every level of study with their co-operations and discussions.

This thesis study and my research period in Coastal Engineering Laboratory at METU become a total pleasure with the aids and cheerfulness of technicians Arif Kayışlı, Yusuf Korkut and research assistants Gökçe Fışkın Arıkan, Hülya Karakuş, Ceren Özer and Gülizar Özyurt.

Everything is less tiresome and more amusing, owing to invaluable motivation, helps, unlimited patience and in fact, *presence* of Irmak Yeşilada.

Hoping that this Masters Degree is going to be a start for an academic career, as successful as my parents', Cihat Şafak and Şükran Şafak. I am lost for words to thank them *for everything I acquired*.

TABLE OF CONTENTS

LIST OF FIGURES

FIGURES

LIST OF TABLES

TABLES

LIST OF SYMBOLS

A_p	sediment dependent scale parameter
B	beach berm height above still water level
B_s	width of an offshore breakwater
BYP	bypassing factor of groin
C_{g0}	deep water wave group velocity
C_Q	calibration coefficient of longshore sediment transport rate
D_{50}	median grain size diameter
D_c	depth of closure
D_{LT}	limiting depth of longshore sediment transport
d	water depth
d_b	wave breaking depth
erf	error function
E	wave energy
g	gravitational acceleration
G	transition distance of an offshore breakwater
GB	distance away from the groin
H_0	deep water significant wave height
H_b	wave breaking height
H_{bd}	modified wave breaking height
$H_{s\text{-}12}$	non-breaking significant wave height, that is exceeded 12 hr./year
H_{tp}	wave height at the tip of breakwater
k	an assigned range to compute occurrence probability of waves
K_d	coefficient of diffraction
K_r	coefficients of refraction
K_s	coefficients of shoaling
l	beach nourishment project length
l_{gb}	groin length from the seaward tip of groin to the breaking location
L_e	efficient length of groin

L_g	length of groin
L_{off}	wavelength at the tip of an offshore breakwater
m_b	beach slope at breaker location
P_i	Occurrence probability of wave with height H_i
PERM	permeability factor
Q	longshore sediment transport rate
Q_{gross}	gross longshore sediment transport rate
Q_{left}	longshore sediment transport rate in left direction
Q_{net}	net longshore sediment transport rate
Q_{right}	longshore sediment transport rate in right direction
$Q(H_i)$	exceedence probability of wave with height H_i
q_y	sources/sinks along the coast
S	offshore distance of an offshore breakwater
t	time
T	significant wave period
V	volume of beach fill per unit length
W	width of beach fill
x	longshore distance
y	offshore distance
y_{LT}	offshore distance of limiting depth of longshore sediment transport
ys	seawall coordinate
Y_o	nourished beach width
α_0	deep water wave approach angle
α_b	wave breaking angle
α_{bd}	modified wave breaking angle
α_{bs}	effective wave breaking angle
α_i	incident wave angle at the seaward tip of the groin
ε	diffusivity
γ_b	wave breaker index
Δt	time increment
Δx	longshore distance increment

PREFACE

Within the scope of this study, a numerical model is developed, based on one-line theory, to calculate shoreline changes due to wind wave induced longshore sediment transport, in existence of coastal structures such as seawalls, groins, T-groins and offshore breakwaters. Main objective of this study is to acquire basic concepts of coastal sedimentation, longshore sediment transport and numerical modeling of resulting shoreline changes under wind waves. Numerical model is applied to an existing case at Bafra in Black Sea coasts of Turkey.

Studies in recent years pay attention on environmentally more friendly methods of shore protection. Therefore, beach nourishment is also discussed by using the numerical model.

To comprehend wave-sediment interaction, an introduction to nature of coastal sedimentation problems is presented in Chapter 1. In Chapter 2, a review of coastal sedimentation studies and history of beach evolution models are given. Fundamentals of one-line theory are discussed in Chapter 3, in details. Introduction of structures and beach nourishment projects into the numerical model as constraints, are explained in Chapter 4, together with basic assumptions and resulting limitations of the model. In Chapter 5, effect of wave data input manner to a shoreline change model is discussed, together with an application in a case study at Bafra. Recommendations for further studies and conclusions are given in Chapter 6.

CHAPTER 1

INTRODUCTION

We will end as sand grains
Equal all in size,
There must be an earth brain
Handling us quite wise.

Angela Kunz

Coasts are projected to be home to at least 3 billion people by 2025 (Finkl, 1996) . Not only by means of their aesthetical beauty in natural life, are coastal zones indispensable also because of their economical potential with eternal resources and expensive investments such as marinas, harbors, quays, etc.

Nearshore processes include several parameters such as waves, currents, tides and also movement of sediments, which affect dynamics of coastal zones significantly. Coastal sedimentation is one of the main concerns of coastal engineering profession since sediment transport cause the movement of shoreline and change in the nearshore bathymetry of coastal zones. Wind wave induced sediment transport takes place in longshore (littoral drift) and cross-shore directions, first of which is taken as the governing pattern in long term shoreline changes and related one-line numerical models. Longshore sediment transport is transport of sediment in parallel to the shoreline, which is assumed to be caused by waves breaking at an angle to the shore and wave induced nearshore current circulation in one-line theory (*Figure 1.1*) .

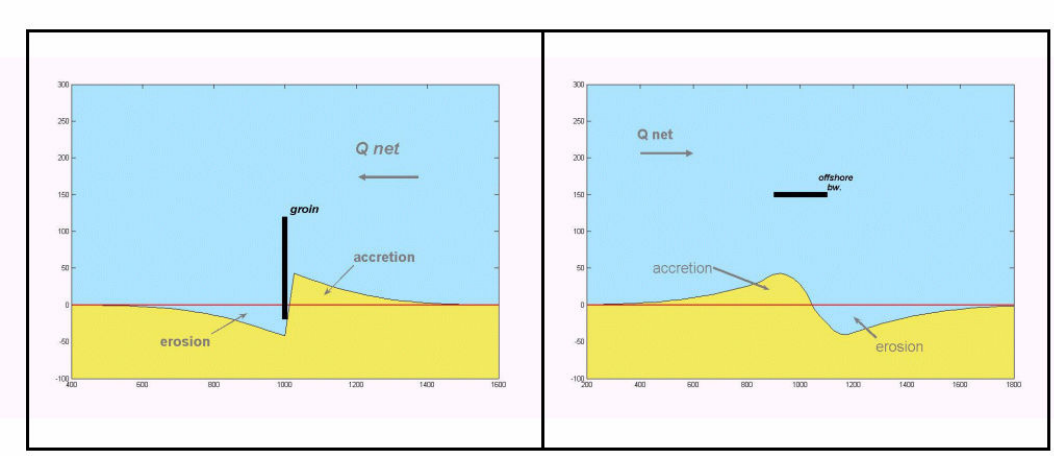

Figure 1.1 Longshore sediment transport

1.1 Wave – Sediment Interaction

Sediment transport may cause erosion, accretion or stability in the shoreline. Erosion is draw-back of the shoreline where opposite, the seaward movement of shoreline, is called accretion. It is estimated that 70 % of the world's sandy shorelines are eroding (Davison et al., 1992), which shows the necessity of considering erosion as an inevitable case and taking measures accordingly. First, causes of erosion need to be summarized as follows (Hanson and Kraus, 1986a):

- Rise in sea level
- Increase in severity of incident waves
- Change in local magnitude and direction of incident waves, which is usually due to construction of a structure in coastal system
- Interruption of drift by structures
- Loss of sediment supply from rivers

Kamphuis (2000) adds *comminution* as a major cause of coastal erosion since coastal zones suffer from uncontrolled decrease in size of beach material as a result of climate changes. In fact, excessive changes in shoreline, no matter it is erosion or

accretion, may cause damage of coastal structures and affect use of coastal zones and resources negatively. Excessive erosion in a coastal system may even damage nearby buildings, highways and other structures. There is a wide but blunder impression that accretion is a less serious problem than erosion. However, construction of an improperly planned groin at kilometers away from a harbour may cause excessive accretion at the updrift side of the breakwater of this harbor, which has several undesired consequences. Similarly, shoaling in inlet channels may prevent safe navigation (Güler, 1997; Güler et al., 1998).

Understanding reasons of coastal sedimentation problems must guide a designer to *react* by taking proper and optimized measures. Since these problems are inevitable in majority of beaches worldwide, and relocating the buildings and infrastructure is terribly wasteful, proper measures are obligatory to minimize their negative outcomes. Any kind of structure on a coastal system may well be defined as a *hard* measure, which provides no protection on adjacent beaches. On the other hand, using sand for shore protection artificially is a *soft* measure. In case shore protection is *certainly* required, the optimum solution alternative should be selected which is well integrated with local processes and cause minimum interruption on natural life and scenery. Accordingly, the coastal system must be well defined with sources, sinks in the system without undermining the coastal scenery, natural life, flora and fauna. Therefore, the first step in a coastal sedimentation study should be that, all structural and soft measures are being assessed well and integrated properly with nature.

Yet, in spite of various efforts, prediction of shoreline changes due to wind wave induced longshore sediment transport and therefore solution of coastal sedimentation problems still contain some uncertainties. Long term morphodynamic response of coastal systems is strongly non-linear with possible limitations on predictability through chaotic behaviour (Southgate, 1995). Dean (1991) considers coastal sedimentation studies on shoreline evolution and beach profile to be a challenge since even only a partial listing of forces on sediments are complicated and difficult

to express with simple examples. Simplifications and basic assumptions are welcome, though they cause some instabilities and errors in results. In order to be able to make comparison among several alternatives and to select the best and most practical solution for sedimentation problems, a consistent numerical model, with relatively lower operating costs, is required as well as physical modeling studies and site investigations. Such a numerical model *has to* provide qualitatively accurate results in the highlight of current studies, *must* be user-friendly and applicable to various boundaries and constraints.

Numerical model, which is developed in this study, transforms (shoaling, refraction, diffraction and breaking) deep water wave characteristics up to the surf zone and calculates shoreline changes due to wind wave induced longshore sediment transport under wide range of inputs and distribution of seawalls, groins, T-groins, offshore breakwaters and beach nourishment projects whose dimensions and locations may be given arbitrarily. The model, eventually, gives the result of shoreline changes with user-friendly visual outputs. Wave data sets are prepared in a separate module, by conducting long term wave statistics. Numerical model is applicable to either a single data set or several data sets. Resulting shoreline, calculated from a data set, is set as the initial shoreline of next data set. Discussion of how to introduce wave data sets into the numerical model is also a major concern.

1.2 Wave Motion

Interaction between waves and sediments is complicated and reveals the necessity to comprehend fundamentals of wave motion initially. *Linear Wave Theory* is widely accepted in coastal engineering applications in order to predict the nearshore characteristics of waves, depending basically on deep water significant wave height (H_0), significant wave period (T) and approach angle (α_0) of incoming waves with respect to shoreline in deep water. Nearshore wave characteristics are determined

making wave transformation computations, i.e. shoaling, refraction, diffraction and breaking, by using these parameters.

Sea bottom starts to affect the wave profile due to the conservation of energy flux at depths shallower than half of the deep water wave length, which is called *wave shoaling*. In a line with shoaling, crest of incoming waves have a tendency to become parallel to bottom contours of the shore as they propagates to shallower depths from deep water which is called *wave refraction*, where incoming waves converge or diverge.

If waves face with a barrier before reaching the shore, characteristics of those waves change within the sheltered zone of this barrier depending on initial wave conditions and properties of this interrupting structure. This process is known as *wave diffraction* and will be thoroughly discussed in Chapter 4.

Separation of water particles from "wave form" under the influence of gravity is called *wave breaking*. Breaking is controlled by *wave steepness,* i.e. by deep water wave height and wave period in deep water medium and by wave height, wave period, sea bottom slope and depth at shallower depths. For a constant wave period, crest particle velocity is proportional to wave height. Thus, crest particle velocity becomes equal to wave celerity with increasing wave heights. At this moment, when this velocity becomes equal to wave celerity, wave becomes unstable and breaks. When a wave breaks, its height decreases and consequently, some of its energy is dissipated due to turbulence and bottom friction and some is reflected back to deep water. However, rest of the energy of breaking wave generates other waves, heat and currents. These currents in the breaker zone are essential for morphological changes in the shoreline.

Longshore sediment transport and resulting shoreline changes under wave motion depend on wave breaking height (H_b) and wave breaking angle (α_b). Therefore, deep

water significant wave characteristics should be transformed into breaking locations including the effects of refraction, shoaling and diffraction. In breaking case, though, Linear Wave Theory is no more applicable. Related calculations should be based on several assumptions and different methods are available (Artagan, 2006). In the numerical model, the following method, demonstrated in CEM(2003), is used to compute the breaking parameters since it includes each deep water wave parameter, H_o , T (C_{g0} =1.56T) and α_o :

$$H_b = (H_0)^{4/5} \times (C_{g0} \cos(\alpha_0))^{2/5} \left[\frac{g}{\gamma_b} - \frac{H_b g^2 \sin^2(\alpha_0)}{\gamma_b^2 C_0^2} \right]^{-1/5} \tag{1.1}$$

where

H_b : wave breaking height

H_0 : deep water significant wave height

C_{g0}: deep water wave group velocity

α_0: deep water wave approach angle

g : gravitational acceleration

γ_b : breaker index

Breaker index (γ_b), ratio of wave breaking height (H_b) to wave breaking depth(d_b) in the surf zone, is assumed as Munk (1949) :

$$\gamma_b = \frac{H_b}{d_b} = 0{,}78 \tag{1.2}$$

CHAPTER 2

LITERATURE REVIEW

2.1 History of Beach Evolution Models

Modeling studies of sedimentation effects in shoreline and nearshore bathymetry of coastal systems are discussed in 3 main titles as shoreline change models, beach profile models and 3-D models. One or more of these models and related theories should be used, depending on the current problem and desired results of the study.

Pelnard-Considere (1956) makes the first one-line based mathematical analysis of *shoreline change* with a given value of sediment transport, assuming that beach profile moves parallel to itself up to a certain depth, beyond which no sediment movement takes place and beach profile remains unchanged in long-term scale. Despite the fact that Pelnard-Considere's solution is derived in existence of a simple boundary, a single impermeable groin, this study provides an inspiration and basic formulae for numerical models of shoreline change and is still a favourable tool to evaluate compatibility of shoreline change numerical models. Hanson (1987) makes a gathering of previous studies and develops GENESIS, which is based on one-line theory and applicable under several boundaries and constraints. Dabees (2000) studies on ONELINE and contributes to this model with new features on how to deal with structures in a shoreline change model.

On the other hand, beach *profile models* deal with short term changes in beach profile, which is caused by cross-shore sediment transport. These models can be regarded as the *complementary* of shoreline change models. Bakker (1968) introduces one more *line* to examine cross-shore sediment transport between two

lines and concludes that rate of cross-shore transport and motion of depth contours is proportional to the deviation of profile slope and equilibrium slope. Despite the fact that beach profile changes are usually associated with monthly or seasonal periods and negligible in long term evaluation, severe storms transport sediment so distant in offshore direction in some extreme cases that, beach profile may not return into its initial form even on yearly basis, which disturbs the validity of the basic assumption of one-line theory. Therefore, including cross-shore transport mechanism into shoreline change modeling of regions where cross-shore transport requires attention, guarantees to give more precise results. Furthermore, beach profile studies should accompany one-line models to evaluate short-term response of beach nourishment projects. Basic theories, related studies and operational cross-shore models are discussed by Roelvink and Broker (1993), in details.

3-D (three-dimensional) models include complex and detailed computations of 3-D hydrodynamic equations and calculation of morphological changes in a 3-D domain. However, these models still fail to give definite results. Besides, one of the main difficulties about 3-D beach change models is the requirement of detailed data for their calibration and verification.

Dabees (2000) develops **NLINE**, a contour line change model which computes 3-D morphological changes by a series of contour lines, in existence of complex beach / structure configurations.

Some recent studies in 2000's argue evaluation of numerical models and drive attention on elimination of errors in those computational tools instead of advancing to more complex levels. Thieler et al.(2000) makes a review of available models, their assumptions and recommend re-examination of beach behavior models without making the models more complex by including more variables. Cooper and Pilkey (2004) criticize deterministic mathematical models to be considered as the *one and only* method available and questionable ability of those models to predict beach

behavior with sufficient accuracy. The need of conceptual approach, based on engineering experiences at both site specific and global scale, is stressed to improve design and assessment of projects. Another important remark made by Cooper and Pilkey is recommending to "go slow and soft" in coastal engineering problems. For instance, an on-site experiment to observe beach behaviour by putting sandbags on shore before constructing a groin may eliminate errors in preliminary design stage.

Eventually, in spite of not being so sophisticated, shoreline change models based on *one-line theory*, are quite promising, if qualitative predictions of wave induced longshore sediment transport and resulting shoreline changes are required particularly. One-line models still come out to be one of the most practical methods which accomplish to optimize accuracy of results, effort and input data required. Developments of one-line model should be emphasized in coastal sedimentation profession, which may even lead to improvements for more sophisticated models in its own constitution.

2.2 Effect of Inputs in Beach Evolution Models

Since coastal sedimentation studies and numerical modeling approaches contain various uncertainties and assumptions, a probabilistic approach would be much worthy than a deterministic approach. To obtain precise results reflecting cases in nature, discussion of effect of inputs does never promise to give exact results but surprises would be less unpleasant in short and long term evaluation of design projects, compared to a deterministic study. Vrijling and Meijer (1992) discuss sensitivity of shoreline change computations depending on variation of sediment and wave parameters. Southgate (1995) makes randomization of available wave data sets to get a band of beach profiles, rather than a single number. In this study, accordingly, effect of sequence and input methods of representative average wave data sets into developed shoreline change numerical model are discussed.

CHAPTER 3

ONE-LINE THEORY

3.1 Introduction to One-Line Theory

Pelnard-Considere (1956) provides analytical solutions of shoreline changes under various cases, in one of which longshore sediment transport trap at updrift side of a single impermeable groin under constant unidirectional wave data, is examined. This analytical solution constitutes the milestone of *one-line theory*. Major assumption of Pelnard-Considere's analytical solutions with a given value of sediment transport rate is that, beach profile is in equilibrium and remains unchanged but only moves parallel to itself (either seaward or shoreward) up to a limiting offshore depth called *depth of closure*, beyond which sediment motion is negligible.

One-line theory implies that all contour lines have similar shapes up to depth of closure, as if there were only one contour line (Kamphuis, 2000). Beach profile changes are usually associated with monthly or seasonal periods and variations of rate of longshore sediment transport, caused only by waves and wave induced currents, is deemed as the major agent in a long-term study of the shoreline change assessment (Hanson, 1987). Therefore, one line theory guarantees to provide precise results for periods in the order of years.

Based on the assumptions that i) beach profile moves parallel to itself and is stable in long term evaluation and ii) sediment transport takes place up to a limiting depth of closure, differential equation defining shoreline movement, called *sediment continuity equation*, is derived as follows, using (x,y) coordinate system in *Figure 3.1* :

$$\frac{\partial y}{\partial t} = -\frac{1}{D_c + B}\left(\frac{\partial Q}{\partial x} + q_y\right) \tag{3.1}$$

where

y : offshore distance perpendicular to shoreline

t : time

D_c : depth of closure

B : beach *berm* height above still water level

Q : longshore sediment transport rate

x : distance along the shoreline

q_y : sources/sinks along the coast

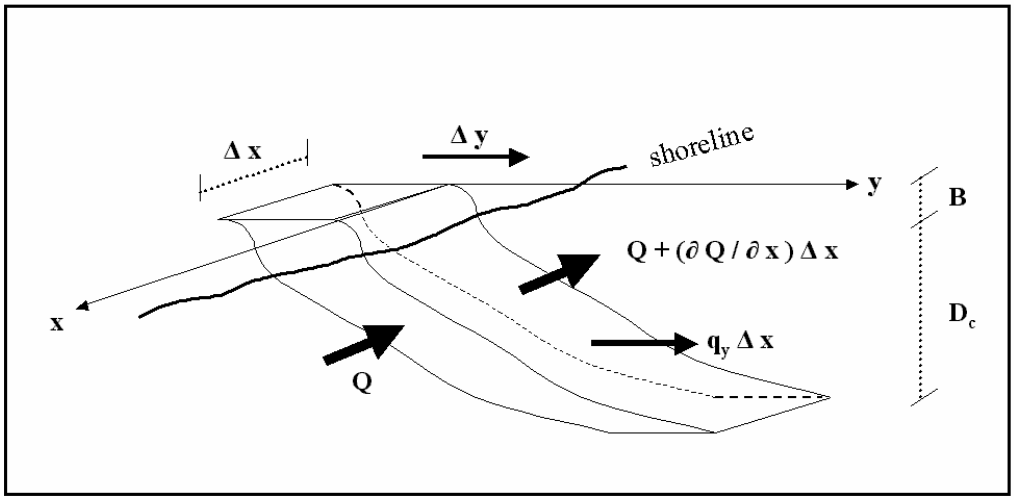

Figure 3.1 Sketch of sediment continuity equation

q_y term indicates constant sources or sinks of sediment in a system. For instance; sediment volume brought by rivers is called a *source* in a coastal system, where sand dredging is simply defined as a *sink* along the coast. Sources or sinks can be defined at arbitrary locations and magnitudes in the developed numerical model.

As being mentioned above, depth of closure (D_c) is a limiting depth, beyond which *sediment motion* is negligible. Hallermeier (1978) presents a wave-climate based computation method, as follows:

$$D_c = 2.28H_{s,12} - \frac{68.5(H_{s,12})^2}{gT^2} \tag{3.2}$$

where $H_{s,12}$ is the height of wave, which is expected to occur for 12 hours in 1 year. This approach makes accurate estimations of *limiting depth of sediment motion* but since longshore sediment transport is taken as the major agent of shoreline changes in the developed numerical model based on one-line theory, it gives overestimated results for *limiting depth of longshore sediment transport.* Accordingly, Hanson (1987) replaces the $H_{s,12}$ term in *Eqn.3.2* with deep water significant wave height (H_{so}) and uses this modified expression to designate limiting depth of longshore sediment transport as D_{LT} , in the one-line model GENESIS. Furthermore, considering that wave breaking is the governing pattern in longshore sediment transport, limiting depth of longshore sediment transport (D_{LT}) is calculated as a function of wave breaking height (H_b) in the developed numerical model, by modifying the expression presented by Hallermeier (1978) in *Eqn.3.2* as follows:

$$D_{LT} = 2.28H_b - \frac{68.5(H_b)^2}{gT^2} \tag{3.3}$$

3.2 Longshore Sediment Transport

Longshore sediment transport is assumed to be caused by waves breaking at an angle to the shore and wave induced nearshore current circulation. Longshore sediment transport takes place in following two manners which are not, in fact, measured separately as easy as they are examined conceptually (CEM, 2003):

- Above the bottom by turbulent eddies of water, which is known as *suspended sediment transport*
- Rolling and saltating close to the sea bed within a layer whose width is function of bed roughness (Bijker, 1971), which is known as *bed load transport*

In comparison, bed load dominates the amount of sediment, transported in longshore direction. *Global* approach, which is based on principle of equilibrium profile, is used to calculate longshore sediment transport rate in one-line theory. In this approach, overall magnitude and direction of longshore sediment transport is calculated, without distinction between suspended load and bed load (Briand and Kamphuis, 1993).

On the other hand, majority of longshore sediment transport takes place in surf zone in offshore distribution. Considering its vertical distribution related to water depth, longshore sediment transport decreases rapidly from sea bottom to still water level (Kraus et al., 1989) .

A sign convention to direction of longshore sediment transport in a particular region at any time should be designated in numerical modeling of shoreline changes. In the developed numerical model, longshore sediment transport is taken as positive in right direction (Q_R) and negative in left direction (Q_L) looking at the seaward. Therefore, net and gross (total) sediment transport rates for a particular region are calculated respectively as:

$$Q_{NET} = Q_R + Q_L \tag{3.4}$$

$$Q_{GROSS} = Q_R + | Q_L | \tag{3.5}$$

Longshore sediment transport rate is expressed either as volume transport rate (Q_l) in m^3/sec or immersed weight transport rate (I_l) in N/sec. Longshore sediment transport

rate can be calculated by various methods such as using tracers or by trapping the moving sediments in coastal zones. In numerical models, the main objective is to obtain an expression, which accounts for the basic necessary parameters and gives accurate results comparing to field data and physical model studies.

Kamphuis (1991) conducts three-dimensional physical model study with regular and irregular waves to obtain a longshore sediment transport rate expression, which includes wide range of effective parameters. In these experiments, beach profile and bottom contours are set to be constant, which is perfectly coherent with the main assumptions of one-line theory. Consequently, non-dimensionalization of parameters is made together with the discussion of experimental results and the following formula is derived:

$$Q = 7.3\, H_{sb}^{2}\, T^{1.5}\, mb^{0.75}\, D50^{-0.25}\, sin^{0.6}(2\alpha_{bs}) \quad (m^3/hr) \qquad (3.6)$$

where

H_{sb} : significant wave breaking height (in m.)

T : significant wave period (in sec.)

m_b : beach slope at breaker location

D_{50} : median grain size diameter (in m.)

α_{bs} : effective wave breaking angle

Compared to previous approaches such as CERC formula (Shore Protection Manual, 1984) derived by energy flux method (Komar,1977), Kamphuis' approach *(Eqn . 3.6)* considers influence of each parameter more accurately, especially influence of wave breaking height, since the formula does not overestimate the effect of wave breaking height for severe storms. Formula, derived by Kamphuis, is preferable in low-wave energy conditions since it gives more consistent predictions for both spilling and plunging breaking wave conditions due to inclusion of wave period in the expression, which has significant influence on the breaker type (Wang

et al., 2002). Therefore, longshore sediment transport rate, Q, is calculated by Kamphuis formula in the developed numerical model. In fact, actual longshore sediment transport rate, valid for long-term evaluation, may be different considering the sources and sinks in a coastal system and therefore, should be computed as a fraction of this potential rate by multiplying with a calibration coefficient, C_Q ($0 \leq C_Q \leq 1$). Besides, the constant of this expression is valid for sand with porosity of 0.32.

3.2.1 Effective wave breaking angle

In one-line model, interaction between incident waves and gradually changing shoreline is taken into account (Hanson and Kraus, 1993). Wave breaking angle (α_b) is modified according to the slope of shoreline at each location as (*Figure 3.2*):

$$\alpha_{bs} = \alpha_b \pm \tan^{-1}\left(\frac{\partial y}{\partial x}\right) \tag{3.7}$$

where α_{bs} is effective wave breaking angle for small values of $\frac{\partial y}{\partial x}$

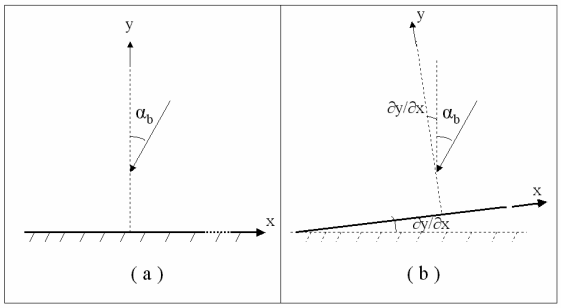

Figure 3.2 Sketch of effective wave breaking angle

3.2.2 Beach profile and beach slope

Beach profile of a coastal system can simply be defined as distribution of depths; d with respect to offshore distance, y. Dean (1991) expresses the shape of the bottom profile as:

$$d(y) = A_p \, . \, y^{2/3} \tag{3.8}$$

where

d : water depth at a distance *y* from shoreline

A_p : sediment dependent scale parameter

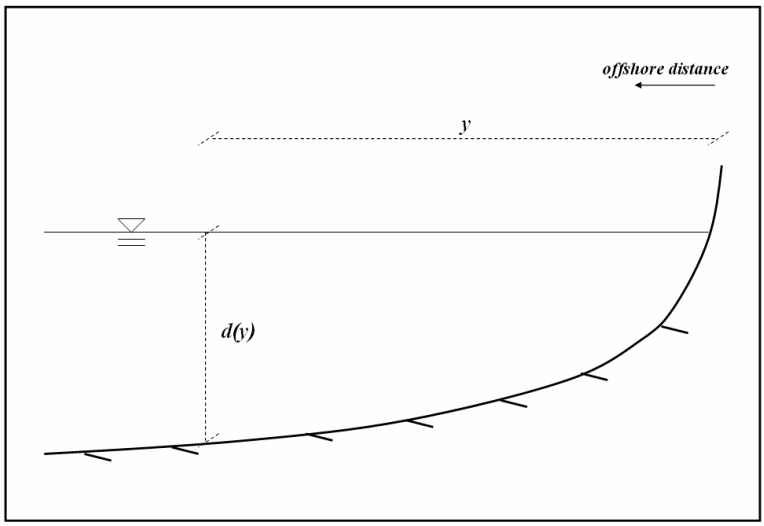

Figure 3.3 Dean Profile

A_p is given as a function of median grain size diameter (D_{50}) as follows (Kamphuis, 2000) :

$$A_p = (1.04 + 0.086(\ln D_{50}))^2 \quad \text{for} \quad 0.1\text{x}10^{-3}\text{m.} \leq D_{50} \leq 1\text{x}10^{-3}\text{ m.} \tag{3.9}$$

Accordingly, beach slope at breaker location (m_b) is calculated in the developed numerical model as follows (Kamphuis, 2000):

$$m_b = \frac{2}{3} A_p^{1.5} d_b^{-0.5} \tag{3.10}$$

where

d_b : wave breaking depth

3.3 Explicit Solution of Sediment Continuity Equation

In the structure of one-line numerical model, instead of analytical solution, sediment continuity equation (*Eqn. 3.1*) is converted to an explicit finite difference scheme depending on longshore distance, y(x,t) and longshore sediment transport rate, Q(x,t) *(Figure 3.4)*. In this scheme, gradual change of longshore sediment transport rate in alongshore direction is calculated by the following expression:

$$\frac{\partial Q_i}{\partial x} = \frac{Q_{i+1} - Q_i}{\Delta x} \tag{3.11}$$

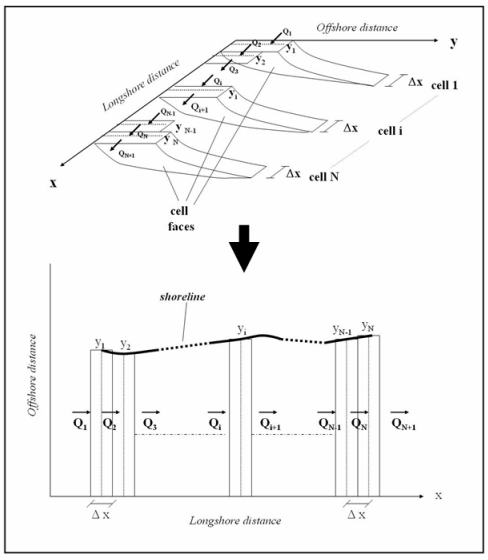

Figure 3.4 Finite difference scheme

Consequently, the expression given below is derived to solve sediment continuity equation explicitly:

$$y_i' = y_i + \frac{\Delta t}{(D_c + B)\Delta x}(Q_i - Q_{i+1} + q_y \Delta x) \tag{3.12}$$

where

Δt : time increment

Δx: longshore distance increment

Subscript "i+1" indicates the next increment in alongshore direction and prime (') indicates values at next time step. Explicit solution of sediment continuity equation using finite difference scheme is described as fixing the shoreline displacements to compute sediment transport rates at the same time step, and fixing sediment transport rates to compute shoreline displacements at the next time step (Dean and Yoo, 1992).

3.3.1 Boundary conditions

Shoreline change numerical models have a control volume and boundaries. In spite of not being mentioned in most of the previous studies, the very first boundary and input of a shoreline change model is the initial coordinates of shoreline. Secondly, observing *Eqn.3.12* and *Figure 3.4* reveals that, number of longshore sediment transport rate expressions is one more than number of shoreline coordinate expressions. Therefore, conditions at ends of control volume must be defined. As initial boundary conditions in the numerical model, longshore sediment transport rates at the boundaries are set as $Q_1=Q_2$; $Q_{N+1}=Q_N$. Other boundaries originate from the existence of coastal structures, which are actually called *constraints*. Fundamentals of modeling of coastal structures as constraints in the numerical model are discussed in Chapter 4, in details. Besides, beach nourishment, which is kept as

the shift of shoreline at certain locations within the applicability of developed numerical model, is also discussed in Chapter 4.

3.3.2 Stability

In the explicit scheme, since shoreline coordinates (y) at $t=t_1+\Delta t$ depend on shoreline coordinates and longshore sediment transport rates at $t=t_1$, stability comes out to be an important parameter. At every time step and longshore distance increment, stability is checked by the following expression:

$$R_s = \frac{Q}{\alpha_b (D_c + B)} \frac{\Delta t}{\Delta x^2} \leq \frac{1}{2} \tag{3.13}$$

In the model, Δx and Δt values are assigned by the user. Taking greater time increments and / or smaller longshore distance increments to solve sediment continuity equation decrease stability of the solution and may cause oscillations in resulting shoreline (Hanson, 1987).

3.4 Implicit Solution

Despite using explicit scheme to solve sediment continuity equation in the developed numerical model, a brief discussion of implicit solution of sediment continuity equation is also introduced. In implicit scheme, different from the explicit scheme basically, gradual change of longshore sediment transport rate in alongshore direction is calculated as follows:

$$\frac{\partial Q_i}{\partial x} = \frac{1}{2}\left(\frac{Q'_{i+1} - Q'_i}{\Delta x} + \frac{Q_{i+1} - Q_i}{\Delta x} \right) \tag{3.14}$$

In the implicit scheme, shoreline coordinates at a certain time are not only dependent on variables of previous time step, but also on those of current time step. Stability is an advantage within implicit solution, whereas the boundaries and constraints in the model become more complex than explicit scheme (Hanson, 1987). In the developed numerical model, *explicit solution is chosen to solve sediment continuity equation* due to the simplicity of introduction of boundaries and constraints, without turning a blind eye to stability of results.

CHAPTER 4

NUMERICAL MODEL

The developed numerical model is applicable to most widely used four coastal defense structures and their complex distributions which are seawalls, groins, T-groins and offshore breakwaters, the first of which have no diffracting but armoring effect on shoreline. In this chapter, introduction of these coastal structures into the numerical model as constraints are presented, together with their basic definitions and design considerations. Beach nourishment, which is simply defined as the advance of shoreline within the applicability of developed numerical model, is also discussed herein. In addition, assumptions and resulting limitations of the numerical model are demonstrated.

4.1 Wave – Structure Interaction and Sediment Motion

Major cause of longshore sediment transport gradients, which result with shoreline changes, is reduction of wave energy reaching the shore due to diffraction, dissipation and reflection effect of coastal stabilization structures in their sheltered zones. Numerical models, based on one-line theory, neglect dissipation and reflection effect of these structures. On the other hand, individual and combined wave diffraction effects of structures and computation of resulting wave breaking heights and wave breaking angles in their sheltered zones require significant attention. Kraus (1984) discusses variation of wave breaking height, H_b, behind an obstacle as a function of diffraction, refraction and shoaling. Behind an infinitely long breakwater on (x,y) plane, where x-axis is placed along the shoreline and y-axis placed perpendicular to the shoreline, wave breaking height at point P (*Figure 4.1*), is computed as:

$$H_b = K_d\,(\theta_D,\, d_b)\;.\; K_r\,(\theta_G,\, d_b).\; K_s(d_b)\;.\; H_{tp} \qquad (4.1)$$

where

H_{tp} : wave height at the tip of breakwater, *T*

K_d , K_r , K_s : coefficients of diffraction, refraction and shoaling, respectively

d_b : water depth at *P*, wave breaking depth.

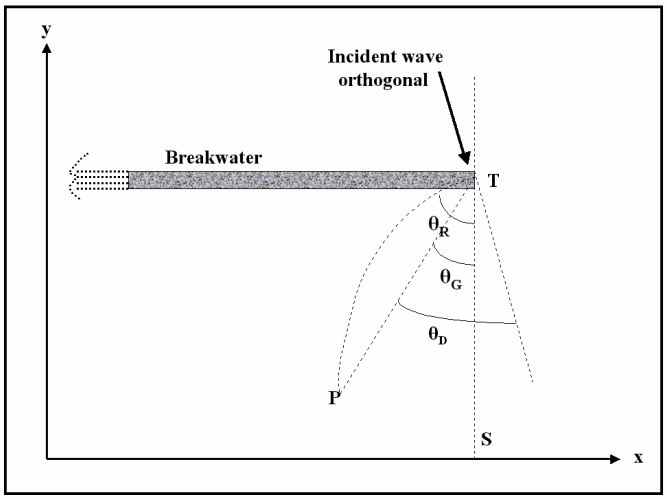

Figure 4.1 Variation of wave breaking height behind an obstacle (Kraus,1984)

According to Kraus, a wave should start with an angle θ_R (greater than θ_G) to arrive and break at point P. This assumption aims to ease the modeling of wave transformation although wave breaking angle is noted to be underestimated. Hanson (1987) uses this approach in GENESIS.

In the numerical model, wave breaking parameters such as wave breaking height (H_b), wave breaking depth (d_b) and wave breaking angle (α_b) are initially calculated within the modeled region. Afterwards, these parameters are modified to account for changes in wave patterns from each diffraction source at the breaking depth d_b, as demonstrated by Dabees (2000):

$$H_{bd} = K_d \cdot H_b \tag{4.2}$$

where

H_{bd} : modified wave breaking height

K_d : diffraction coefficient

4.2 Groins

Groin (groyne) is the most common, long and narrow coastal stabilization structure, built usually perpendicular to shore (*Figure 4.2*) in series (Kamphuis, 2000). A groin is constructed to interrupt longshore sediment transport - partially or completely – in order to retard erosion at a certain location, to prevent the alongshore transported sediment from entering a harbor or an inlet or to retain fill within a project area.

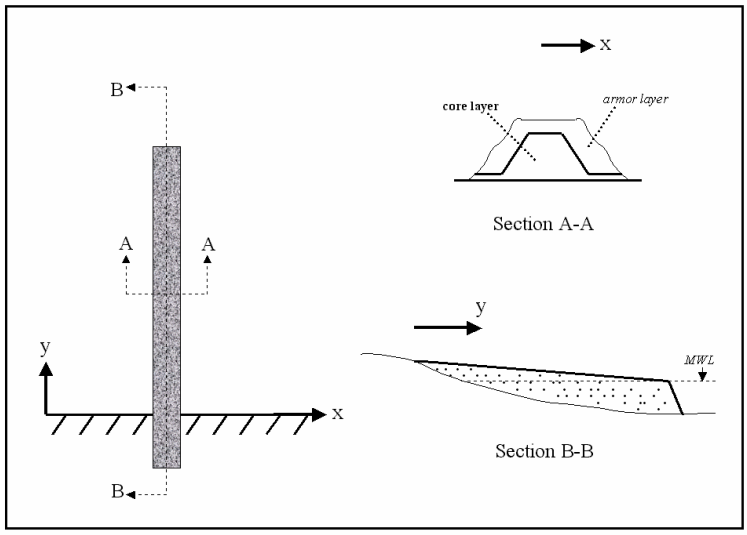

Figure 4.2 Sectional views of a groin

On the other hand, groins have *almost no effect to reduce offshore sediment transport* and may even enhance this movement due to rip currents. Therefore, if cross-shore transport is dominant in a region, offshore breakwaters should be considered first. In general, groins must be preferred in coastal zones where net longshore sediment transport is relatively low in order to achieve the balance

between the sides of groin. In fact, a groin must block littoral transport only to the extent necessary to preserve the design beach cross section, while allowing the net ambient net littoral transport to bypass the structure to downdrift beaches. Lower limit of offshore design length of a groin is given in Beach Management Manual (1996) that it exceeds breaker line for moderate design wave parameters. On the other hand, proper functioning of groins in series requires spacing around 2-3 times of length of groins (SPM, 1984). Beach Management Manual (1996) provides detailed information about basic design concepts of groins, the comparison of required construction materials, capabilities, and disadvantages etc.

4.2.1 Groin constraint in the numerical model

In the numerical model, shoreline-perpendicular groins, with arbitrary locations, offshore lengths and permeability ratios, could be placed. Groins, which do not pass the breaker line in seaward direction, are assumed to have *no diffracting effect on breaking waves but only have sediment trapping capacity* as simple barriers. On the other hand, wave breaking parameters in sheltered zones of groins which are passing the breaker line in seaward direction, need to be highlighted.

As being mentioned, Dabees (2000) initially calculates wave breaking parameters such as wave breaking height (H_b), wave breaking depth(d_b) and wave breaking angle(α_b) in the sheltered zones of structures, as if there is no diffraction-causing effect. Afterwards, these parameters are modified at locations under the effect of diffraction sources. Kamphuis(2000) made a regression analysis for wave diffraction and diffraction coefficients near structures, based on the diffraction method for random seas (Goda et al., 1978), as a function of angle (θ) between incident wave ray at groin's seaward end and an arbitrary point (*Figure 4.3*) and the formula given in *Eqn.4.3* is derived.

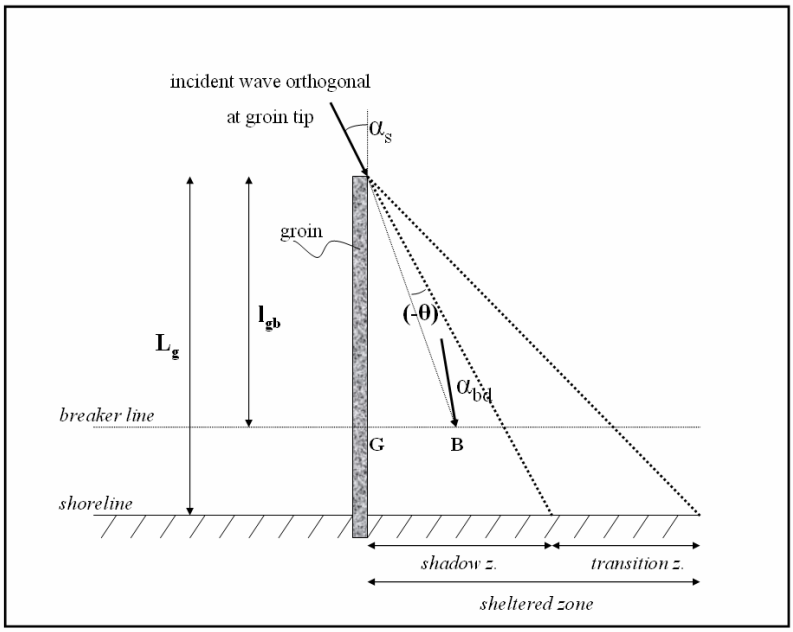

Figure 4.3 Diffraction of waves near a groin (Kamphuis, 2000)

$$K_d = 0.71-0.0093\ \theta+0.000025\ \theta^2 \quad \text{for } 0 \geq \theta > -90 \tag{4.3}$$

To compute diffraction coefficients in the transition zone, the trend of diffraction coefficient in the shadow zone is linearly extended up to the end of sheltered zone (Baykal, 2006). Then, the modified wave breaking height (H_{db}) is computed as follows:

$$H_{bd} = H_b \,.\, K_d \tag{4.4}$$

where

H_{bd} : modified(by diffraction) wave breaking height

K_d : diffraction coefficient for this particular location

On the other hand, wave breaking angle in the sheltered zone of groins is calculated by the method demonstrated by Dabees (2000) as a function of diffraction coefficient:

$$\alpha_{bd} = \alpha_b \cdot K_d^{0.375} \tag{4.5}$$

where

α_{bd} : diffracted wave breaking angle

α_b: (undiffracted) wave breaking angle

Inside the shadow zone, however, a further decrease in the breaking angle is taken into account as:

$$\alpha_{bd} = \alpha_b K_d^{0.375}\left[\frac{2GB}{l_{g_b}\left(\tan\alpha_i + \tan(0.88\alpha_b)\right)}\right] \quad \text{if} \quad \frac{GB}{l_{gb}} < \frac{1}{2}\{\tan(\alpha_i) + \tan(0.88\cdot\alpha_b)\} \tag{4.6}$$

where

l_{gb} : groin length from the seaward tip of groin to the breaking location

α_i : incident wave angle at the seaward tip of the groin

GB: distance away from the groin

In fact, the effect of a groin in a coastal system as a structure and in the numerical model as a constraint, is formulated as the ratio of transport rate passing the groin to the rate arriving to the updrift (Hanson, 1987) . Two major concerns about ratio of transport rate passing a groin are *bypassing* around the groin and *permeability* of the groin.

4.2.2 Bypassing

Bypassing is the indirect movement of sediment around tip of a groin, occurring if groin fails to reach up to depth of closure at any instant. Bypassing factor of a groin (BYP) is volumetric ratio of bypassed or in other words *permitted* volume of sediment, to the total volume of sediment reaching the updrift of that groin.

Physically, groins with filled updrift, cause less damage on downdrift side. Otherwise, long groins, which are not filled but interrupt longshore transport, will cause more severe erosion. Offshore currents due to sea level rise, severe storms and the groins themselves, may cause loss of accreted region on updrift side. Offshore moved sediments are coarser material which is hard to be brought back (Kamphuis, 2000). This case causes instability on sides of groin and consequently more erosion on downdrift. In nature, a portion of bypassed material around groins, usually starts to accumulate at the tip of groin as soon as bypassing starts(*Figure 4.4*), which requires cross shore evaluation of sediment transport. A numerical model based on one-line theory does not manage to visualize this concept. Instead, bypassed volume of sediment is directly added to the downdrift of groin.

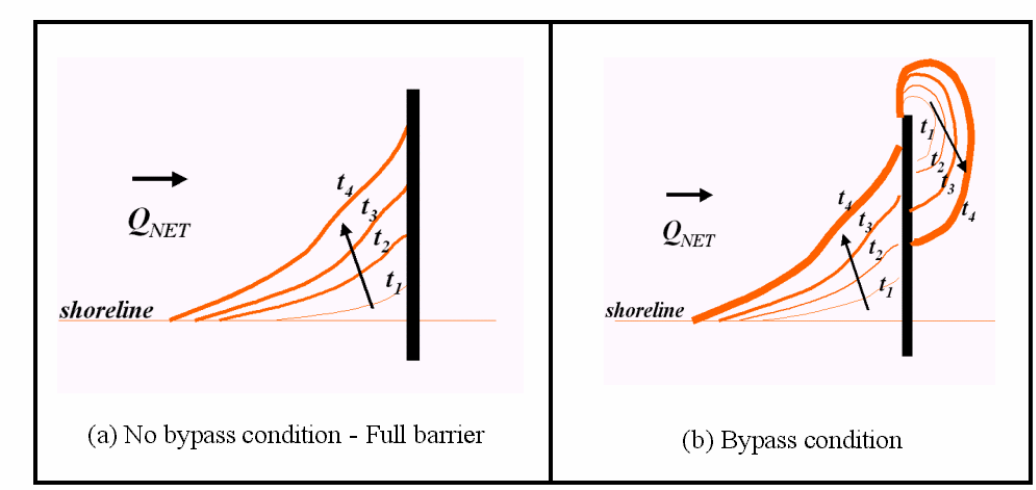

Figure 4.4 Bypassing around groins in nature

Hanson (1987) calculates bypassing factor of a groin in GENESIS, which is based on one-line theory and takes longshore sediment transport as the governing pattern, as:

$$BYP = 1 - \frac{D_g}{D_{LT}} \tag{4.7}$$

where D_g is depth at seaward end of groin. If groin passes limiting depth of longshore sediment transport ($D_g > D_{LT}$), this expression is set to zero. In this approach, assuming a planar profile with a uniform slope gives a more realistic bypassing factor as:

$$BYP = 1 - \left(\frac{D_g}{D_{LT}} \right)^2 \tag{4.8}$$

In the developed numerical model, effective length and therefore sediment trapping capacity of a groin is kept time dependent. Accordingly, effective length of a groin is adjusted as follows due to accretion or erosion:

$$L_e = L_g - y_{groin} \tag{4.9}$$

where y_{groin} is the accumulation distance of sediment at updrift side and L_g is the length of groin. Kamphuis (2000) demonstrates the following formula to calculate bypassing factor of a groin at a beach, whose bottom profile is expressed by *Dean profile* (*Eqn.3.8* & *Fig.3.3*):

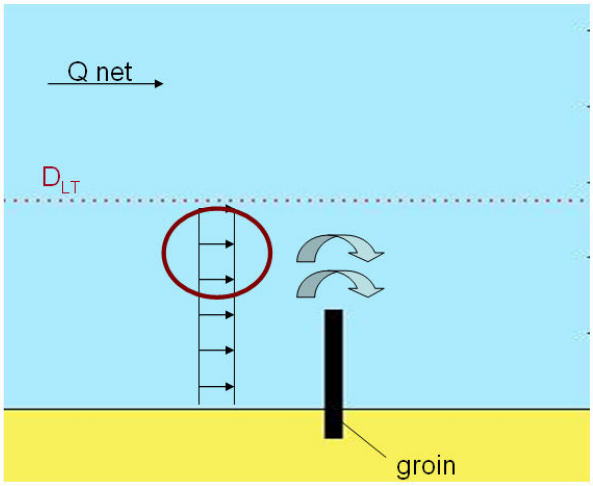

Figure 4.5 Aerial view of bypassing around tip of a groin

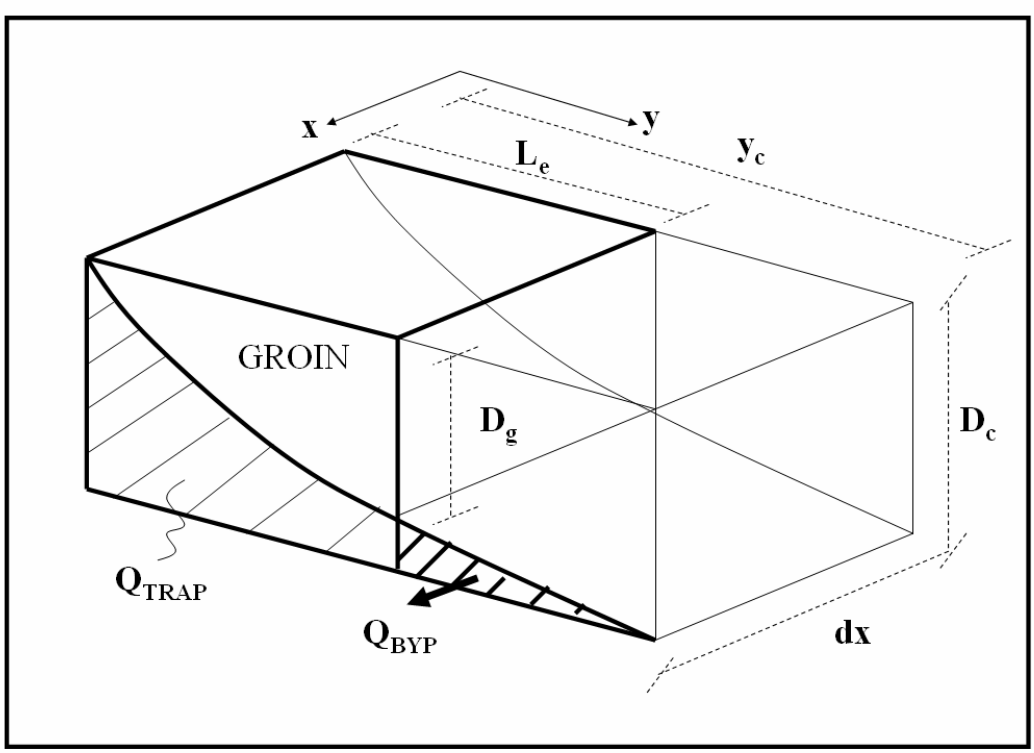

Figure 4.6 Bypassing around tip of a groin (Kamphuis,2000)

$$BYP = 1 - \frac{L_e D_c - 0.6 A_p L_e^{5/3}}{y_c D_c - 0.6 A_p y_c^{5/3}} \tag{4.10}$$

where

L_e : effective length of groin

y_c : offshore distance of depth of closure

Depth of closure(D_c) expression in this formula is replaced by limiting depth of longshore sediment transport (D_{LT}), computed by *Eqn.3.3* and similarly, y_c is set to be the offshore distance of limiting depth of longshore sediment transport (y_{LT}) , since developed numerical model accounts for longshore sediment transport and resulting shoreline changes. Therefore, bypassing factor is calculated as follows:

$$BYP = 1 - \frac{L_e D_{LT} - 0.6 A_p L_e^{5/3}}{y_{LT} D_{LT} - 0.6 A_p y_{LT}^{5/3}} \quad (4.11)$$

If groin reaches to limiting depth of longshore sediment transport ($L_e = y_{LT}$), above expression becomes zero:

$BYP = 0$ for $L_e \geq y_{LT}$

Secondly, if a groin is filled to its capacity and effective groin length, L_e, becomes zero, bypassing ratio becomes 1, which means loss of function of a groin with total bypass of sediment to updrift. However, filling to capacity is possible only if a long-term unidirectional flow exists.

$BYP = 1$ for $L_e = 0$

4.2.3 Permeability

Permeability is a more stable concept than bypassing and defined as permission of a structure to pass sediment through. Permeability of a coastal structure is usually discussed as a single coefficient, PERM, combining *overtopping* and *transmissivity*, the first of which is a function of crest height and the latter is the existence of gaps within the structure.

4.2.4 Bypassing and permeability in the numerical model

Ratio of sediment volume reaching downdrift to cumulative sediment volume at updrift is given as a whole, PB, in GENESIS (Hanson, 1987) and ONELINE (Dabees, 2000) as follows:

$$PB = BYP + PERM - BYP \,.\, PERM \quad (4.12)$$

where BYP is bypassing factor and PERM is the single coefficient of permeability. Hanson (1987) distributes this permitted volume of sediment by adding at downdrift in GENESIS as:

$$Q_G = PB.\ Q_{G\pm1} \tag{4.13}$$

where subscript G indicates updrift location in front of groin and G±1 indicates downdrift of groin. In the developed numerical model, longshore sediment transport rate at downdrift of groin is set to be this cumulative bypassed and transmitted volume. In fact, this *first grid* logic is acceptable for bypassing within the limitations of one line theory as long as the modification of diffraction coefficients and breaking angles are made in case of permeable groins.

Within the structure of numerical model, wave breaking heights and wave breaking angles are computed in the sheltered zone of groins, firstly assuming impermeable and full barrier groins where the only parameter is their offshore lengths. Dabees (2000) modifies diffraction coefficients and wave breaking angles at downdrift of groins as a function of the permeability of this structure, as follows:

$$K_{dP} = K_d\ (1\text{-PERM}) + \text{PERM} \tag{4.14}$$

$$\alpha_{dP} = \alpha_d\ (1\text{- PERM }) + \alpha_b\ \text{PERM} \tag{4.15}$$

Initially calculated diffraction coefficients and wave breaking angles in the sheltered zone of groins remain same in existence of an impermeable groin (PERM=0) . On the other hand, a totally permeable *theoretical* groin (PERM=1) equalizes diffraction coefficients to 1 and diffracted wave breaking angle to initially computed wave breaking angle, α_b. This approach is adapted in the developed numerical model to calculate diffraction coefficients and wave breaking angles in sheltered zones of groins by considering their permeability.

4.2.5 Model tests

Simulations are made in the numerical model separately to test permeability and bypassing of sediment volumes at groins, using unidirectional wave data. First, bypassing is tested on an initially straight shoreline, y=0, with an impermeable groin of 100 m. Resulting shorelines at miscellaneous times are shown in *Figure 4.7*.

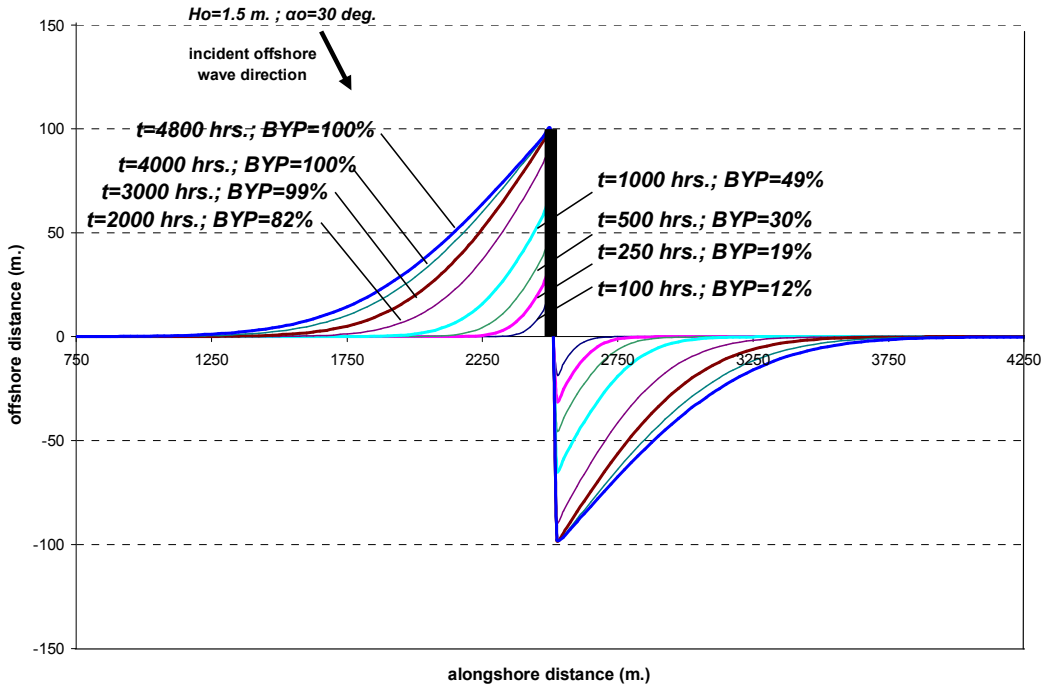

Figure 4.7 Bypassing around an impermeable groin on an initially straight shoreline

Rate of accretion at updrift face of groin decreases with time, as an expected cause of increasing bypassing. After 3000 hours of wave action, updrift side of groin is filled to its capacity and sediment volume starts to be bypassed and accretion is observed not at *updrift of groin*, but far from the groin. Similarly, downdrift erosion becomes stable and fixed nearby the groin, following the total bypass of material reaching at updrift. As being mentioned before, filling to capacity is possible only if such a long-term unidirectional flow exists.

Secondly, a groin with an offshore length of 200 m., is placed on an initially straight shoreline, y=0. The initial offshore length of groin is set to prevent bypassing (BYP=0) throughout the simulations. Results for varying values of permeability of the groin are given in *Figure 4.8*.

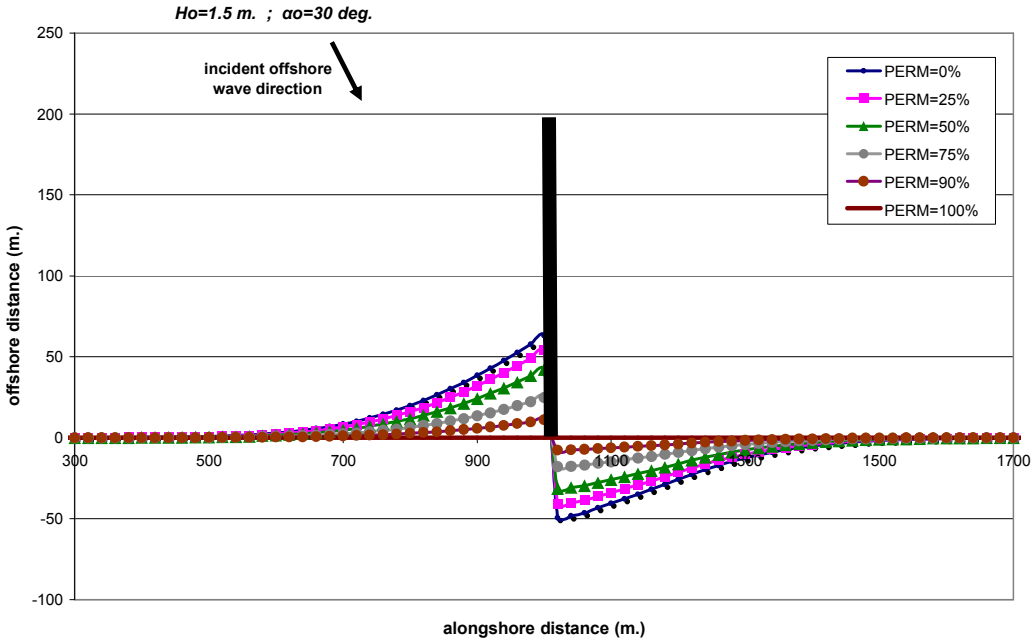

Figure 4.8 Permeability of a single groin on an initially straight shoreline

A fully impermeable groin causes the maximum accretion and erosion at updrift and downdrift respectively. As the permeability of groin increases, severities of both accretion and erosion decrease. Eventually, a fully permeable (PERM= 100%) groin gives the same results with the theoretical *no groin* case.

To investigate the joint applicability and effects of bypassing and permeability, a 100 m. groin is placed on initially straight shoreline. Deep water significant wave height is again kept as 1.5 m with deep water approach angle of 30^{o}. Shoreline changes after 1000 hours are given below, for varying permeability coefficients (PERM).

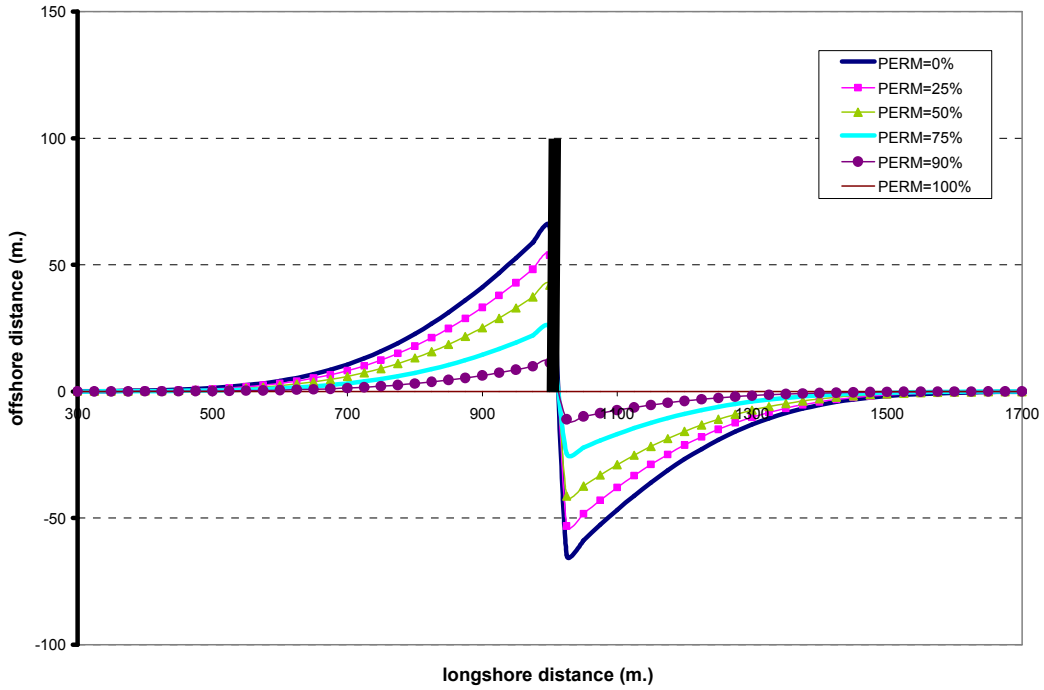

Figure 4.9 Permeability of a single groin, bypassing sediment

Permeability of a groin which allows sediment to bypass (*Figure 4.9*), has en effect in the same order with permeability of a groin which do not permit sediment bypassing around its tip (*Figure 4.8*). Therefore, bypassing and permeability, which are two major concerns of longshore sediment transport in existence of groins, are consistently set in the developed numerical model.

The above discussions reveal that, groins with filled updrift cause less damage on downdrift side. Besides, permeable groins mitigate downdrift erosion. As long as each individual shoreline change case is discussed site-specifically, lengths of groins must be adjusted properly to allow or prevent bypassing and permeable groins may be preferred in design to achieve optimum serviceability from these structures.

4.3 T-Groins

T-groins can be defined as the conjunction of a shore perpendicular groin and a shore parallel offshore breakwater. The purpose of adding a breakwater section to a groin is to diffract wave energy before reaching shoreline. Besides, T-groins provide functional improvements to conventional groins due to reduction of rip currents and blockage of offshore movement of sediment near groins (CEM, 2003).

4.3.1 Offshore breakwaters

Offshore (detached) breakwaters are usually built parallel to shoreline, to which they have no solid connection. Despite the fact that offshore breakwaters have higher construction and maintenance costs compared to groins, they have attractive features, not shared by groins, such that they weaken longshore currents but do not deflect them offshore and they block offshore movement of sediment in their lee (Hanson and Kraus, 1991) .

However, unless fill material is placed to adjacent beaches during construction of offshore breakwaters, downdrift erosion is inevitable similar to groins. Suh and Dalrymple (1987), McCormick (1993) and Hsu and Silvester (1990) discuss shoreline changes in the vicinity of offshore breakwaters, caused by transport of this eroded material. In the numerical model, shoreline parallel offshore breakwaters with arbitrary permeability, locations, widths and distances from shoreline could be placed together with segmented breakwaters with gaps in between. Offshore breakwaters, which do not pass the breaker line in seaward direction, are assumed to have no diffracting and naturally no shoreline change effect.

Wave motion and therefore computation of wave breaking parameters in sheltered zone of offshore breakwaters are more challenging than those of groins. (*Figure 4.10*)

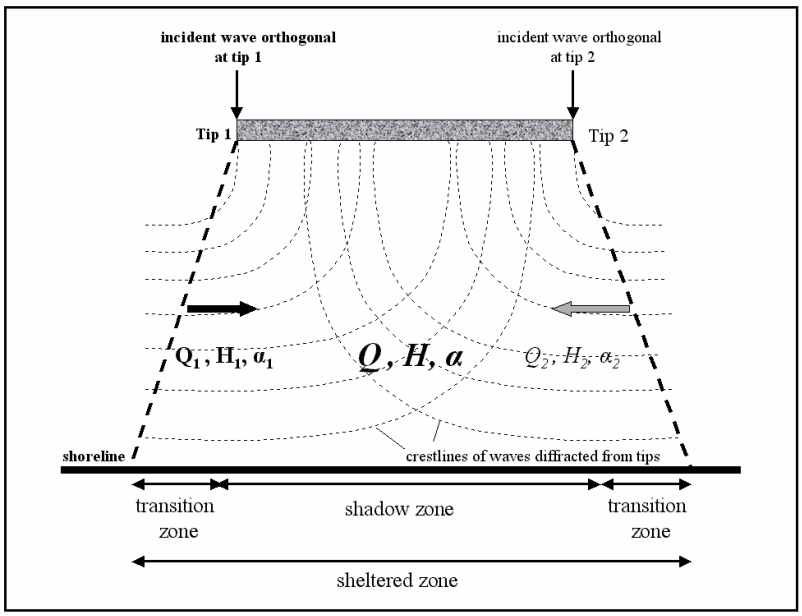

Figure 4.10 Diffraction effects behind an offshore breakwater (Dabees, 2000)

Wave breaking angles are modified under diffracting effects in sheltered zones of offshore breakwaters using the methodology demonstrated by Dabees (2000). In the vicinity of offshore breakwaters, wave breaking heights (H_b) are modified similar to sheltered zones of groins. Regression analysis of Kamphuis (2000), given in *Eqn 4.3,* to calculate diffraction coefficients are also used, in the shadow zone of offshore breakwaters. The trend of diffraction coefficient in the shadow zone is linearly extended within the transition zone (*Figure 4.9*). The modified wave breaking height, H_{bd}, is again computed by *Eqn.4.4.* Following the separate clarification of wave breaking angles and wave breaking heights from both tips separately, the resultant wave breaking height and wave breaking angle at an arbitrary point are calculated by regarding dominancy of the tip, close to this arbitrary point (Artagan, 2006).

4.3.2 T-Groin constraint in the numerical model

A T-groin can be introduced into the developed numerical model *manually*, by defining a groin and an offshore breakwater separately. Certainly, offshore length of groin must be same with the seaward distance of breakwater from shoreline and location of groin section must be *within the alongshore range* of offshore breakwater. In this study, shoreline-perpendicular groin sections of T-groins are taken as impermeable barriers. Therefore, in the vicinity of T-groins*, resultant* wave heights and wave breaking angles are *not* computed alike the case in an offshore breakwater. Instead, wave breaking parameters are computed at both sides of groin separately and diffraction effect of effective tip is taken into account up to the full barrier section behind the offshore breakwater section (*Figure 4.11)***.** Other considerations of diffraction behind the breakwater section of T-groins are totally same as offshore breakwaters.

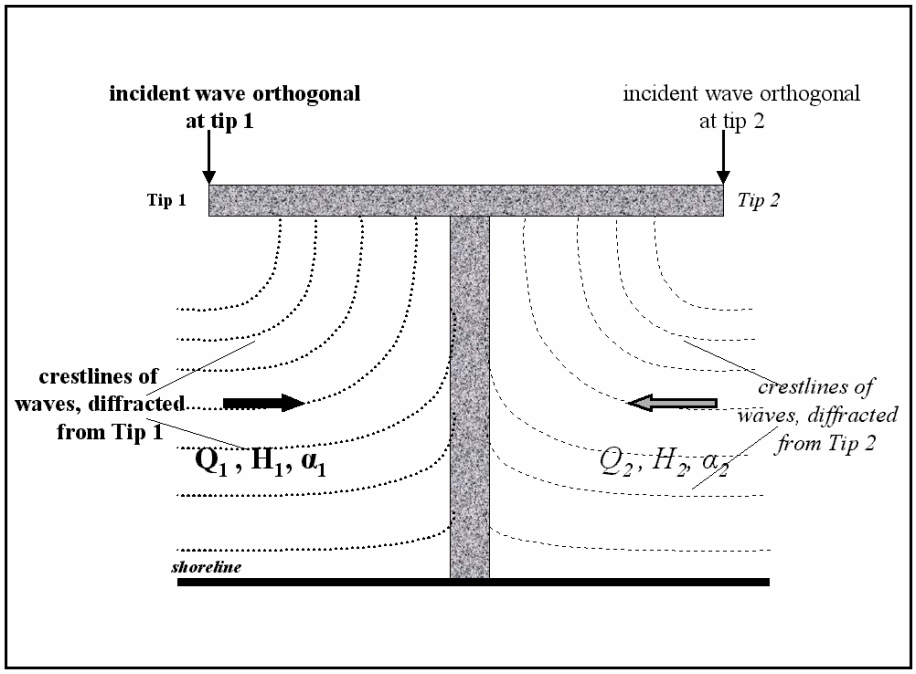

Figure 4.11 Diffraction effects behind a T groin

This assumption provides applicability not only for perfectly symmetrical T-groins, but also for sections with groins which do not touch offshore breakwater at the middle and for L-groins (*Figure 4.12*). L groins are especially considerable for the evaluation of erosion - accretion problems in harbor projects.

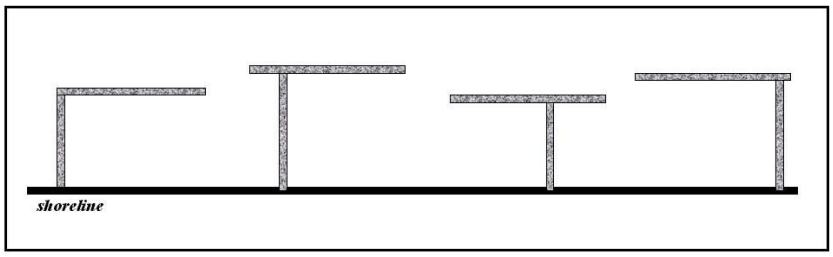

Figure 4.12 Possible sections modeled by methodology of T-groins

In consistency with the assumptions for groins and offshore breakwaters, T-groins which do not pass the breaker line in seaward direction, are assumed to have no diffracting effect but only sediment trapping capacity, alike groins.

4.4 Seawalls

One of the major intentions of constructing seawalls, as coastal armoring structures, is to protect inland areas from flooding. In fact, any revetment, breakwater or bulkhead can be regarded as *seawall*. In the developed numerical model, seawall is considered as a barrier, built on shore at an arbitrary landward distance from shoreline, to prevent sediment transfer between in front of it and behind its boundaries.

4.4.1 Seawall constraint in the numerical model

In the numerical model, shoreline parallel seawalls with arbitrary locations, widths and landward distances from shoreline can be placed in the model. Basic boundary condition, which is defined to include the effect of a seawall into a shoreline change model is that *the beach fronting the seawall can not move landward of it* (*Figure 4.13*). When shoreline reaches a seawall at a particular location, sediment can not originate from that area. There can be gain, but no loss at this location (Hanson and Kraus, 1986a). Numerically, this condition is defined as:

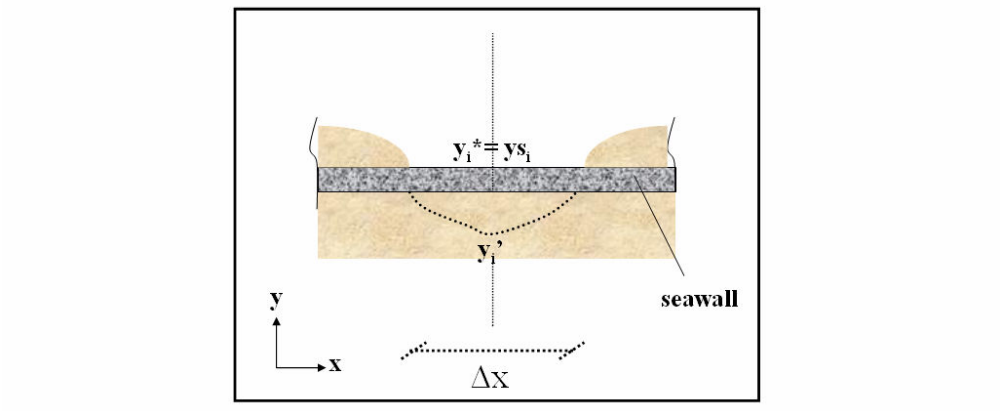

Figure 4.13 Basic shoreline correction on i'th grid at seawall constraint

$$y_i^* = ys_i \tag{4.16}$$

where

ys_i : seawall coordinate at i'th grid

y_i' : computed shoreline coordinate at next time step (*Figure 4.12*)

y_i^* : modified shoreline coordinate at next time step

In earlier studies, longshore sediment transport is set to zero where shoreline reaches the boundaries of a seawall (Ozasa and Brampton, 1979). Hanson and Kraus (1986a)

argue that, sediment volume must be conserved by adjusting longshore sediment transport rates to values that will place the shoreline at the seawall by discussing grid cells as minus, plus and regular areas (*Figure 4.14)* .

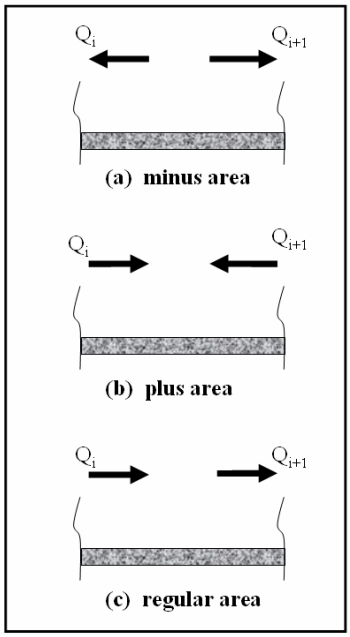

Figure 4.14 Sketch of minus, plus and regular areas (Hanson and Kraus, 1986a)

Correction at a minus cell is as follows:

$$Q_i^* = Q_i \frac{y_i - ys_i}{y_i - y_i'} \tag{4.17}$$

$$Q_{i+1}^* = Q_{i+1} \frac{y_i - ys_i}{y_i - y_i'} \tag{4.18}$$

Correction at a regular cell is as follows:

$$Q_{i+1}^* = Q_i - \frac{ys_i - y_i}{\left(\frac{\Delta t}{2D_c \Delta x}\right)} \tag{4.19}$$

"i" and "i+1" indicates grid numbers in alongshore distance, "*" indicates modified values of longshore sediment transport rates, and " ' " indicates values at next time

step. Since a plus cell is defined to have influx from both of its ends, no receding from seawall is possible and therefore no correction is required.

4.4.2 Model test

Capability of the developed numerical model, to simulate effects of a seawall, is tested by placing a seawall on eroding downdrift side of a groin. Simulations in this section are made by using 1 m. of deep water significant wave height with deep water approach angle of 25^{o}. First, shoreline changes after 1000 hours are calculated in existence of the 150 m. long groin without a seawall (*Figure 4.15*).

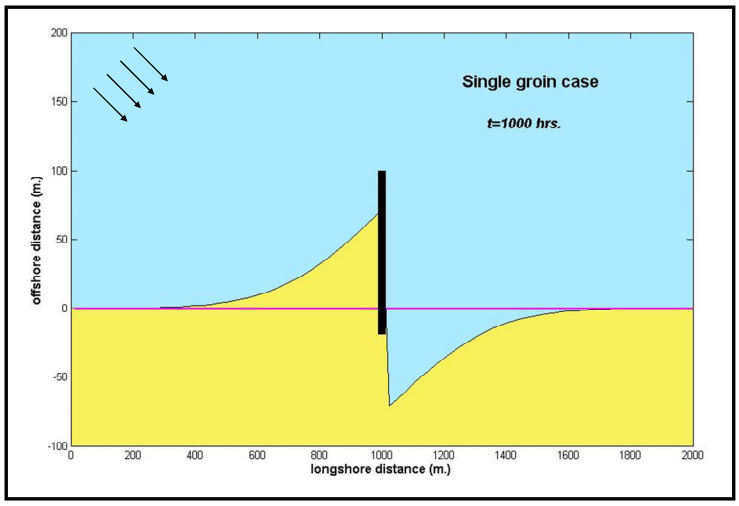

Figure 4.15 Single groin case (t=1000 hrs.)

Secondly, a seawall of width 300 m. is placed at downdrift of this groin and 25 m. landward from the initially straight shoreline. Shoreline changes at t=75 hours, t=250 hours, t=750 hours and t=1000 hours are given in *Figure 4.16*.

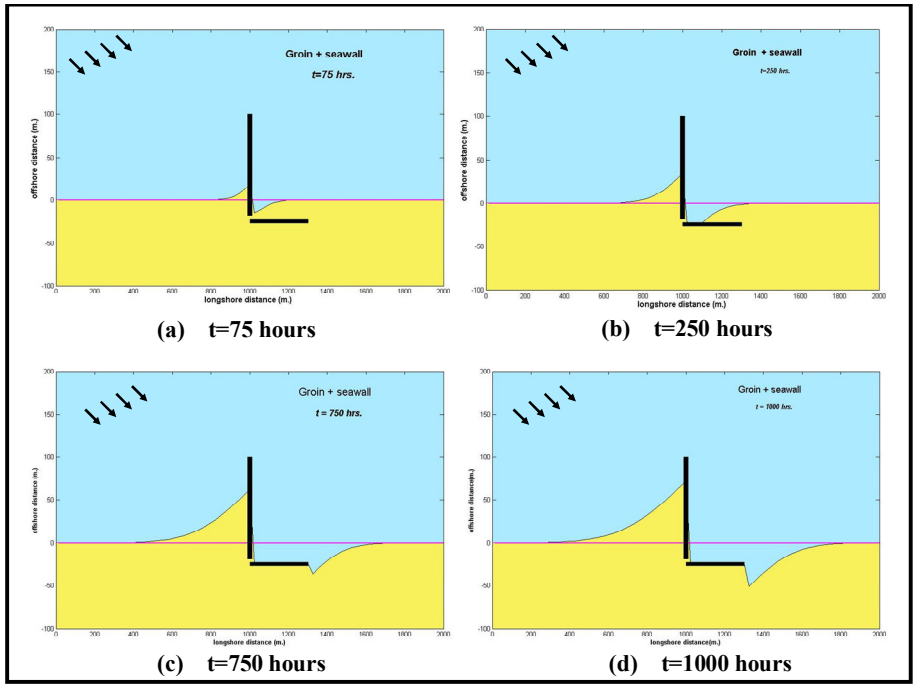

Figure 4.16 Groin + seawall case

Resultant shoreline changes after 1000 hours for both cases, with and without seawall, are given below:

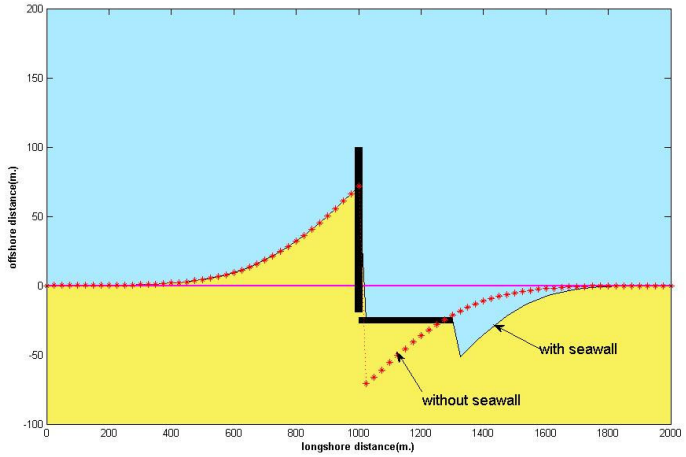

Figure 4.17 Comparison of single groin case and groin + seawall case

As being observed from *Figure 4.17*, seawall has naturally no effect on accretion at downdrift side of groin. On the other hand, existence of seawall at downdrift side prevents the *drastic* erosion. However, this restricted volume causes the erosion, beyond the boundaries of seawall, to be much severe. Therefore, sediment loss is not prevented and roughly, no advantage is obtained in cumulative evolution alike the other hard coastal measures.

4.5 Beach Nourishment

Beach nourishment (beach fill; beach replenishment), which is environmentally most friendly method with least (not *no*) impact on natural life, is the artificial addition of suitable quality sediment to a beach area that has a sediment deficiency, in order to rebuild a beach of width providing shore protection and recreation area (Kamphuis, 2000). Beach nourishment has several attractive features such as, this soft measure is more flexible and do not cause downdrift erosion (Davison et al., 1992). Besides, artificial nourishment of beaches, which requires proper renovation, is relatively more economical than equivalently resulting structural measures. Finkl(1996) exposes that certain Atlantic coasts of U.S. may disappear in few decades without nourishment. Dean (1991) states that alongshore transported material in beach nourishment projects is not regarded to be *lost* and continues to provide benefits at adjacent beaches. Although coastal stabilization structures are criticized to be responsible from downdrift erosion of adjacent beaches and not to add sediment to the control volume (Hall and Pilkey, 1991), groins and offshore breakwaters can be used in conjunction with beach nourishment to increase project longevity, retard fill erosion and reduce re-nourishment costs. Basic design considerations of beach nourishment projects and shift from hard to soft shore protection measures are presented in CEM (2003).

Despite the fact that nourishment is said to be a *soft* measure, it is also interference to natural life and scenery. One of the major disadvantages of nourishment is that a

nourished beach does not *have to* response same as its natural state since it may erode faster and may not recover in long-term basis. Therefore, a nourishment project must be integrated well with its environment, which is achieved by proper assessment of protection, available budget and proper renovation and maintenance of nourishment.

Looking from one line theory point of view, beach nourishment is *widening of beach and advance of one-line (shoreline)* to dissipate more wave energy. Shift of shoreline within a certain range result with a nourished beach in rectangular shape. However, in general, transition sections called tapers, are added to ends of beach nourishment projects in order to mitigate end losses on project integrity. This impact of tapers is more significant if taper width exceeds the value that is 0.25 times the project length (Walton, 1994). Other advantages of these tapers are that they decrease the aesthetical disturbance of rectangular fills on coastal scenery and prevent the lagoonal enclosure of dead water spaces. Hanson and Kraus (1993) analyze economics of beach nourishment projects, placement of transition sections and conclude that an optimization and economical evaluation of design are strictly required. *Figure 4.18* presents an illustration of a beach nourishment project with length l, offshore distance Y_o and taper width, b-a . Independent from the tapers, ratio of nourished beach width (Y_o) to project length (l) is generally in the order of 0.02 at most (Dean and Yoo, 1992).

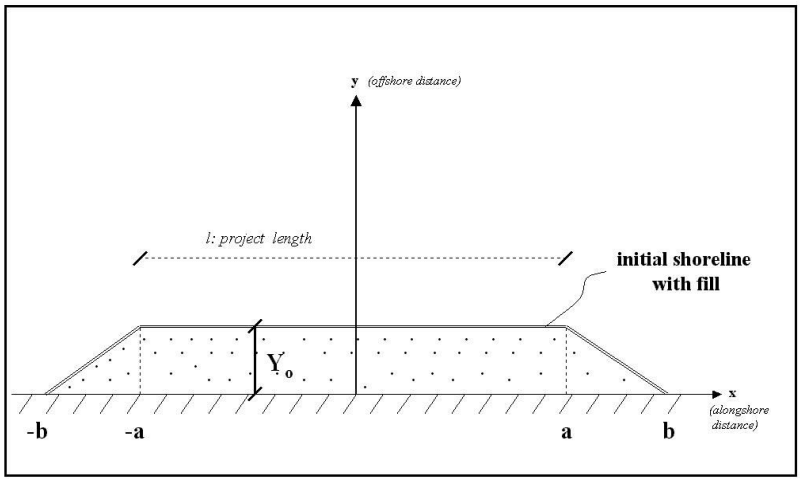

Figure 4.18 A typical tapered beach nourishment project

Behaviour of a nourished beach is dependent on characteristics of fill material. Ideally, using coarser material than native sediment is always trustworthy to obtain a properly protected and wider beach. Depending on the variation between grain size diameter of native and fill sediment, different resulting profiles may occur (Dean, 1991) . In the equilibrium of median grain size of native and fill sediment sizes, the case is rather simple by considering a nourishment project as a shift along the whole profile(*Figure 4.19*), which is going to be discussed in the scope of this study.

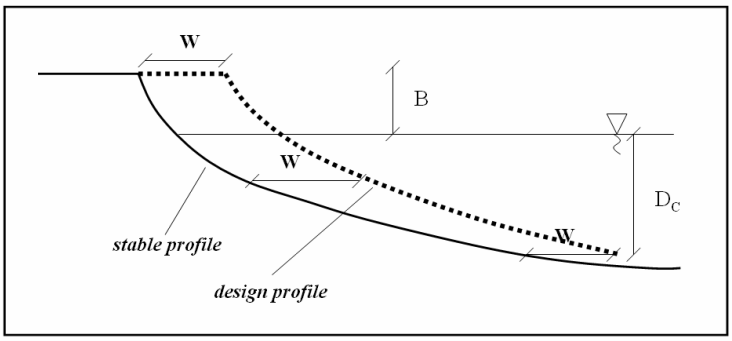

Figure 4.19 Theoretical profile after beach nourishment using native sediment as fill material

In this theoretical profile, volume of beach fill per unit length is roughly estimated as:

$$V=W(B+D_c) \tag{4.20}$$

where V is volume per unit length, W is width of beach fill, B is berm height and D_C is depth of closure.

4.5.1 Beach nourishment in the numerical model

In the developed numerical model, beach nourishment projects, with arbitrary locations, widths, offshore distances from shoreline and taper lengths, can be placed. In the scope of this study, applicability of the shoreline change numerical model to a single nourishment project is studied free from cycles of re-nourishment, and *in the equilibrium of median grain size of native-fill sediment sizes*. Besides, it is assumed that no background erosion takes place. As being mentioned above, beach nourishment is simplified as *advance of one-line (shoreline)* in offshore direction at given locations depending on dimensions of project *(Figure 4.18)* as if the initial shoreline is not straight but irregular. Rough but qualitatively accurate estimate of destination of a nourished beach material under wind wave effects is useful to assess adjacent beach impacts resulting from nourishment, in conjunction of structures with nourishment projects.

4.5.2 Comparison with analytical solution of tapered beach fill

The results of the numerical model are compared with analytical solution of shoreline change in a beach nourishment project to achieve a benchmarking. Walton (1994) presents analytical solution for tapered beach nourishment projects in the coordinate system in *Figure 4.18*, as follows:

$$\frac{y(x,t)}{Y_o} = k_1 + k_2 + k_3 + k_4 + k_5 \tag{4.21}$$

$$k_1 = \frac{1}{2}\left[erf(AX + A) - erf(AX - A)\right]$$

$$k_2 = \frac{1}{2}\left(\frac{B - AX}{B - A}\right)\left[erf\left(AX - A\right) - erf(AX - B)\right]$$

$$k_3 = \frac{1}{2}\left(\frac{B + AX}{B - A}\right)\left[erf\left(AX + B\right) - erf\left(AX + A\right)\right]$$

$$k_4 = \frac{1}{2\sqrt{\pi}(B - A)}\left\{\exp\left[-\left(AX - B\right)^2\right] - \exp\left[-\left(AX - A\right)^2\right]\right\}$$

$$k_5 = \frac{1}{2\sqrt{\pi}(B - A)}\left\{\exp\left[-\left(AX + B\right)^2\right] - \exp\left[-\left(AX + A\right)^2\right]\right\}$$

where

$$A = \frac{a}{2\sqrt{\varepsilon t}}$$

$$B = \frac{b}{2\sqrt{\varepsilon t}}$$

$$X = \frac{x}{a}$$

erf : *error function* , which is computed by programming softwares

Analytical solutions for shoreline change are developed assuming small wave breaking angles (α_b), and the following planform shoreline change equation can be derived (CEM, 2003) , considering the x-y coordinate system in *Figure 3.1* :

$$\varepsilon \frac{\partial^2 y}{\partial x^2} = \frac{\partial y}{\partial t} \tag{4.22}$$

ε is defined as diffusivity (m^2/sec) and calculated as :

$$\varepsilon = \frac{2Q_o}{(D_c + B)} \qquad (4.23)$$

where

$$Q_o = \frac{Q}{\sin 2\alpha_b} \qquad (4.24)$$

A beach nourishment project of 1000 m. length (l) with 500 m. tapers (b-a) at both ends and extending 25 m. in offshore direction (Y_o) is placed on an initially straight shoreline. Simulations are made for 1 year, by taking unidirectional wave data with deep water significant wave height, H_o=1 m. and deep water approach angle, α_o=5°. Analytical and numerical results are presented below:

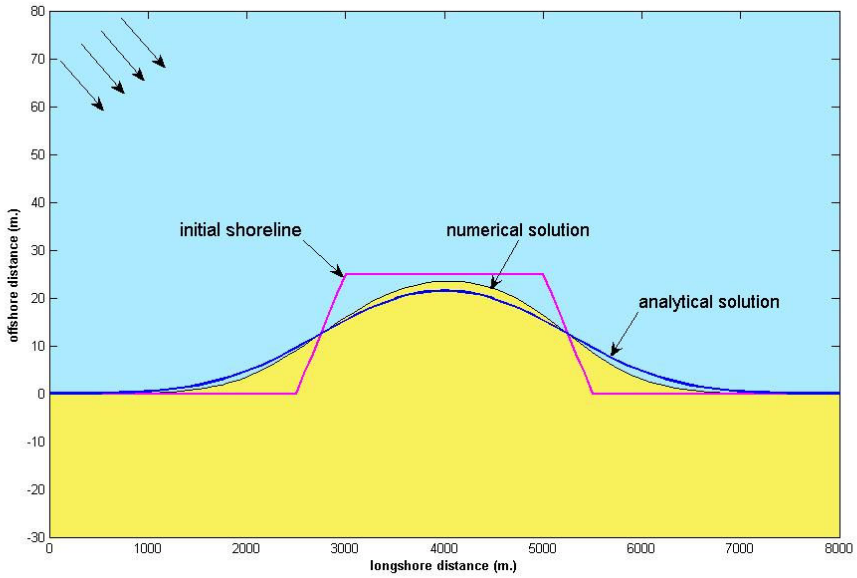

Figure 4.20 1 year analytical and numerical solutions of beach nourishment

Results of the developed shoreline change numerical model are in good agreement with results of analytical solution at the end of 1 year. Therefore, beach nourishment is added as a module in the numerical model, which is applicable on initially straight shorelines.

Including cross-shore sediment transport into the model will improve the reliability of results in this module.

4.6 Assumptions and Limitations of the Numerical Model

One-line theory and shoreline change numerical models based on this theory are promising to give *qualitatively* accurate results with optimum effort and time. However, assumptions and limitations of each independent numerical model should be presented well in order to know the applicability and error range of the model and finally to obtain a convenient evaluation of shoreline changes. Basic assumptions of developed shoreline change numerical model, some of which are already discussed, are given below:

- Sediments are characterized only by their median grain size diameter, D_{50}.
- Linear Wave Theory and relevant approaches are used to define wave motion and transformation.
- Wave breaking parameters are initially calculated within the modeled region and then modified to account for changes in wave patterns from each diffraction source.
- Beach profile is assumed to move in parallel to itself up to the limiting depth of closure.
- Beach bottom shape is defined by *Dean Profile* (*Eqn.3.3*).
- Wind wave induced longshore sediment transport is taken as the governing agent of shoreline changes.
- *Sediment continuity equation* is solved explicitly, using *Finite Difference Scheme*. Longshore sediment transport rates at the ends of the modeled regions are set as $Q_1=Q_2$, $Q_{N+1}= Q_N$ initially, where N is number of increments in alongshore distance.
- Offshore gains or losses in control volume are neglected.
- Dissipative and reflective effects of structures are neglected.
- Diffracting effects of offshore breakwaters which do not reach to a sufficient distance seaward from the breaker line, are neglected.

- Groins and T-groins, which do not pass the breaker line in seaward direction, are set to have no diffracting effect on breaking waves but do only have sediment trapping capability, depending on their length.
- The beach, fronting a seawall, can not move landward of it.
- A beach nourishment project, where median grain sizes of native and fill sediment are equal, is defined as advance of shoreline in offshore direction at certain locations.

CHAPTER 5

A CASE STUDY

In this chapter, the developed numerical model is tested with a case study in Black Sea coasts of Turkey. Besides, effect of method and sequence of wave data input in a shoreline change model is discussed.

5.1 Wave Data Input in a Shoreline Change Numerical Model

Wave data sets are among the basic inputs of shoreline change models. Wave data sets, which represent wave climate of a region for certain duration, are usually preferable to actual wave time series data due to their ease to be handled. These approaches, although straightforward, are also noted to be quite demanding on computer time (Hanson et al., 2003). In the model, therefore, a matrix with 4 columns (deep water significant wave height, significant wave period, deep water approach angle-direction, frequency) is presented as wave data input. Simulations are made using these unidirectional wave data.

In such an approach, wave chronology, in other words input sequence of wave events becomes essential since morphodynamic response of coastal systems is strongly non-linear (Southgate, 1995). In the development of shoreline change numerical models and execution of simulations, resulting shoreline of each wave data set is defined as the initial shoreline of simulation with next wave data set. Varying order of a wave data set means varying its *resulting shoreline*, its successor wave data set and initial shoreline for this successor set. Coastal sedimentation and modeling of sediment transport include complex processes physically and several assumptions numerically, one within the other. Appending uncertainties of monochromatic wave data different

than actual wave time series to those coerce the discussion of input method and sequence of wave data sets.

Southgate (1995) discusses effects of wave chronology on seabed and beach levels by dividing 4 month wave data set into several segments. Combinations are created between these segments to achieve a randomization and consequently a probabilistic approach to yield statistical results of beach levels under wave effects. Güler et al. (1998) use annual and seasonal wave data sets and observe no significant difference on the shoreline evolution obtained by the annual and seasonal wave data. Discussion of effect of wave sequence on shoreline change numerical models with several methods in details, still remains as a question for further studies. In the application of the developed shoreline change numerical model, different methods of wave data input are discussed in the case study.

5.2 Definition of the Problem

Kızılırmak River, the longest river in Turkey, discharges into Black Sea where it forms *Bafra Delta (Figure 5.1)* Resulting from the construction of flow regulation structures on Kızılırmak River, coastal erosion up to 30 m. per year, takes place in this region mostly due to the reduction of sediment budget. A shore protection system with 2 Y-shaped groins and 1 I-shaped groin is designed and constructed as being shown in *Figure 5.2* (Kökpınar et al., 2005). Measured field data before and after construction of these coastal structures (April 1999 – January 2003) are obtained from General Directorate of State Hydraulic Works (DSI) to be used in this case study.

Figure 5.1 Location of Bafra Delta

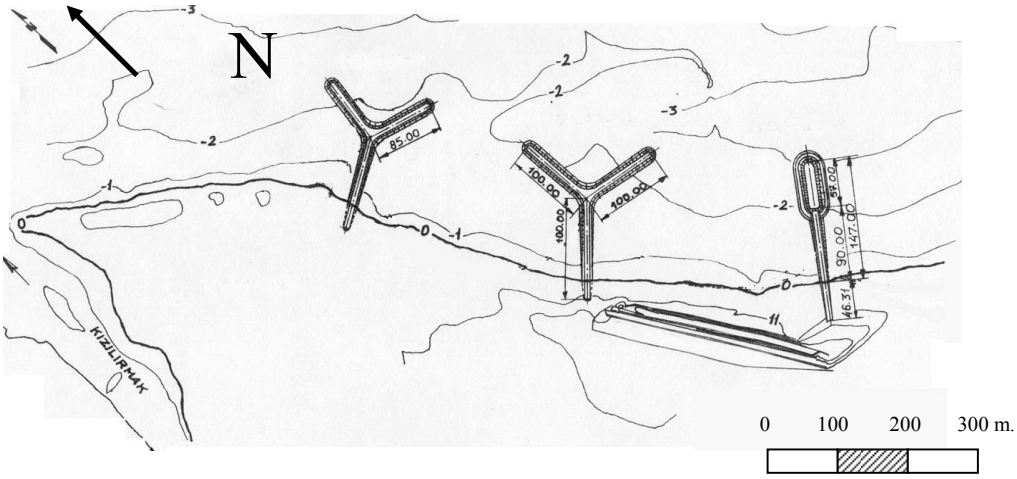

Figure 5.2 Final layout

5.3 Wave Hindcasting

For the application of the numerical model, wave data sets are obtained from local wind data. Wind data, measured at the closest meteorological station at Sinop *(Figure 5.1)* between 1966-1985, are obtained from General Directorate of Meteorological Affairs. Measuring the fetch distances from the related navigation map of Navigation, Hydrography, Oceanography Department of Turkish Navy, shows that Bafra is open to waves approaching from North-West(NW),North-North-West(NNW),North(N),North-North-East(NNE),North-East(NE), East-North-East (ENE),East(E), and East-South-East(ESE) (*Figure 5.3*). On the other hand, due to the geographical cape-structure of the region, a refraction analysis is made which reveals that waves from West-North-West (WNW) direction are also effective in Bafra region and therefore, this direction is also taken into consideration in modeling of shoreline changes. Waves from this direction are introduced to approach nearly perpendicular in deep water, with respect to the shoreline in Bafra. Fetch directions are shown in *Figure 5.3* and effective fetch distances are given in *Table 5.1*.

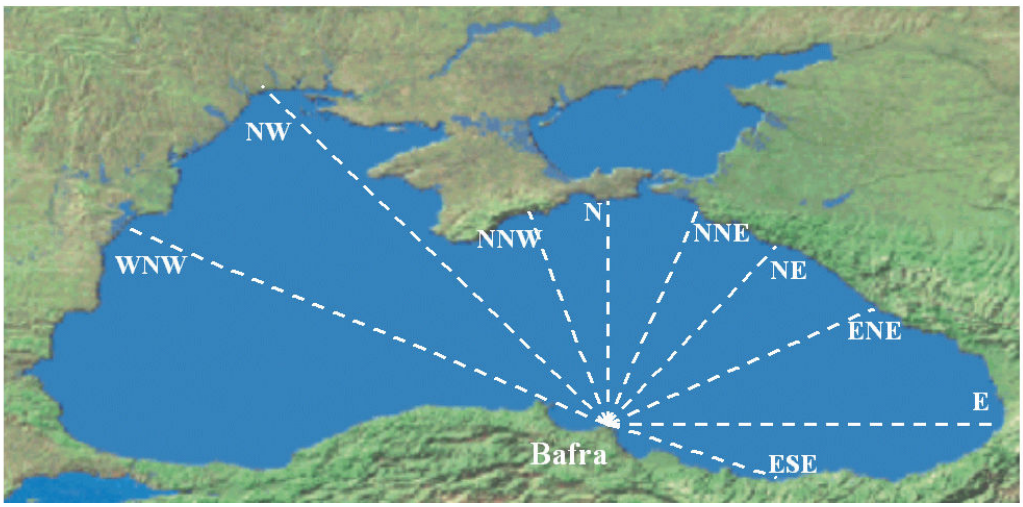

Figure 5.3 Fetch directions at Bafra

Table 5.1 Effective fetch distances

Direction	Fetch Distance (km.)
WNW	617
NW	502
NNW	373
N	330
NNE	331
NE	333
ENE	382
E	349
ESE	282

Hourly average wind data sets are converted to independent storms assuming winds with velocities greater than 3 m/sec as *storm* condition. Using these storm data and fetch distances for each direction, log-linear annual probability equations are derived and presented in *Table 5.2*. Probability distribution of deep water significant wave heights are given for wave directions WNW, NW,NNW, N in *Figure 5.4(a)* and for wave directions *NNE, NE,ENE, E, ESE* in *Figure 5.4(b)* .

Table 5.2 Log-linear annual probability equations of wave directions

Direction	Log-Linear Probability Equation
WNW	$(H_{1/3})_0 = -1.055 \ln Q((H_{1/3})_0) - 0.437$
NW	$(H_{1/3})_0 = -0.788 \ln Q((H_{1/3})_0) + 0.016$
NNW	$(H_{1/3})_0 = -1.056 \ln Q((H_{1/3})_0) - 1.485$
N	$(H_{1/3})_0 = -0.498 \ln Q((H_{1/3})_0) - 0.379$
NNE	$(H_{1/3})_0 = -0.762 \ln Q((H_{1/3})_0) - 1.703$
NE	$(H_{1/3})_0 = -0.588 \ln Q((H_{1/3})_0) - 1.384$
ENE	$(H_{1/3})_0 = -0.522 \ln Q((H_{1/3})_0) - 1.254$
E	$(H_{1/3})_0 = -0.485 \ln Q((H_{1/3})_0) - 0.993$
ESE	$(H_{1/3})_0 = -0.894 \ln Q((H_{1/3})_0) - 0.835$

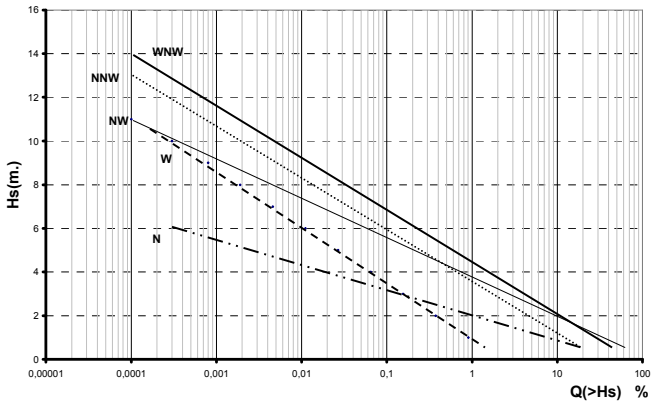

(a)

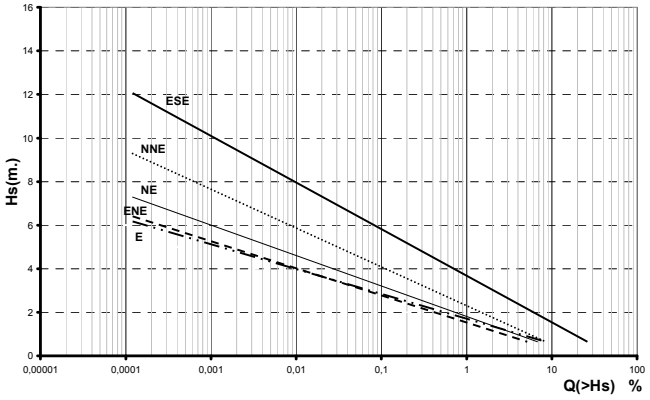

(b)

Figure 5.4 Probability distribution of deep water significant wave heights

5.4 Model Wave Data

In one-line models, wave data input is among the most important parameters affecting the results. In this study, effects of smaller but more frequent waves are considered to be more appropriate to use rather than higher waves with less frequency. In this respect, a concept of average wave height, based on a probabilistic approach, is developed. Thus, for each direction separately, average deep water significant wave height (H_{so}) is computed as (Güler, 1997; Güler et al., 1998):

$$H_{so} = \frac{\sum (P_i . H_i)}{\sum P_i} \tag{5.1}$$

where

H_i : wave height

P_i : occurrence probability of wave with height H_i

Occurrence probability (P_i) of wave with height H_i is computed by using the corresponding frequencies within a given range as follows:

$$P_i = Q(H_i - k) - Q(H_i + k) \tag{5.2}$$

where Q( ) : exceedence probability

k : an assigned range to compute occurrence probability

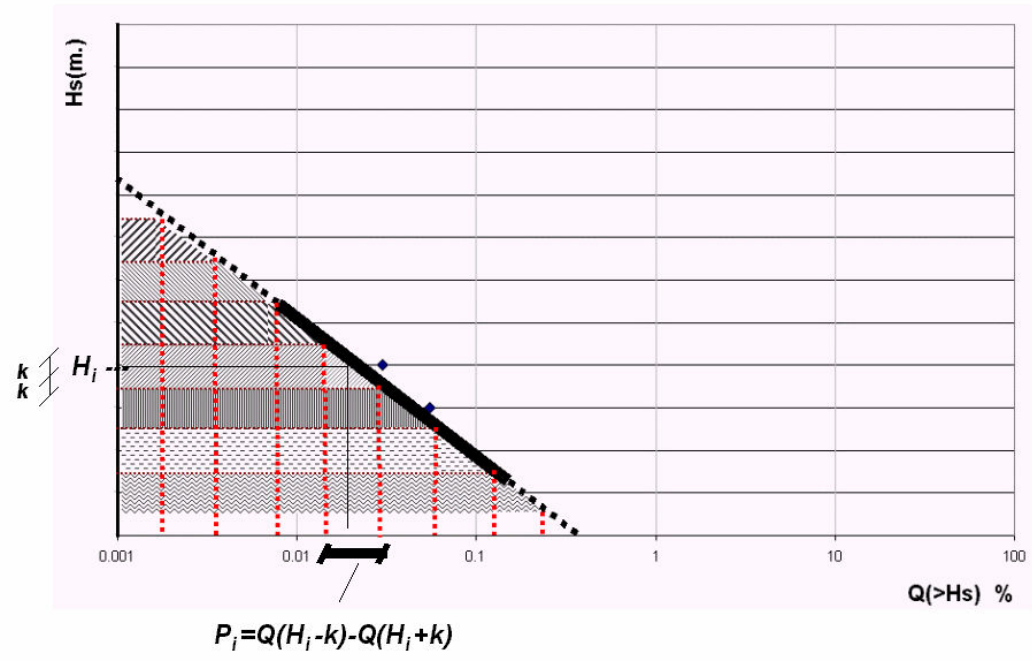

Figure 5.5 Average wave data

Using this method, average deep water significant wave heights are derived for each direction at Bafra. Average deep water wave steepness in Bafra region is calculated as 0.042 from extreme wave statistics (*Figure 5.6*), which is consistent with the value given by Ergin and Özhan (1986) and thus, significant wave period is calculated as:

$$T = 3.91\ (H_s)^{1/2} \tag{5.3}$$

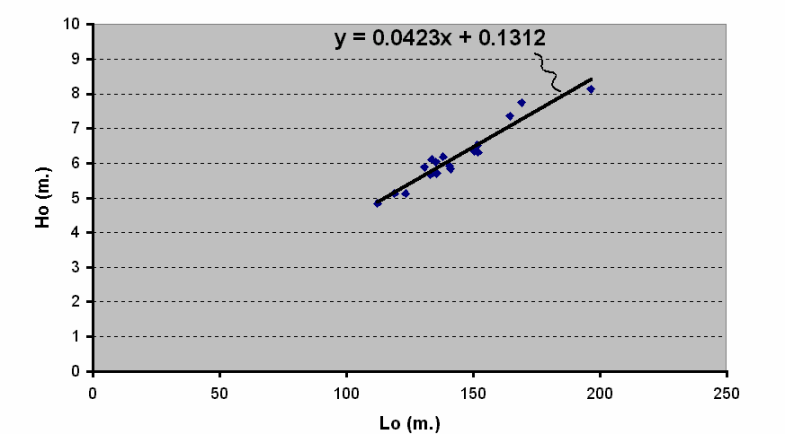

Figure 5.6 Average deep water wave steepness at Bafra

As a result of long term wave statistics, wave data sets (average deep water significant wave heights, significant wave periods and annual exceedence frequencies) of each direction, which are used as wave data input of the shoreline change model, are derived from statistics of past wave climate including 20 year wave data and given below in *Table 5.3*.

Table 5.3 Average wave heights, corresponding periods and annual exceeding frequencies at Bafra

	H(m.)	T(sec.)	f(hrs.)
WNW	1,53	4,83	1365
NW	1,26	4,40	1798
NNW	1,53	4,83	507
N	0,99	3,89	562
NNE	1,24	4,35	185
NE	1,07	4,05	134
ENE	1,01	3,93	114
E	0,98	3,87	151
ESE	1,37	4,57	746

5.5 Wave Data Input Methods

Due to the fact that actual wave time series data are not used in the developed numerical model, input manner of average wave data sets (*Table 5.3*) is investigated. Time interval between two field measurements is 4 year, which is sufficiently long, and therefore, using seasonal wave data is not discussed. Such a discussion can be useful in shorter simulations such as 1 year (Baykal, 2006).

Using annual wave data given in *Table 5.3*, numerical model runs are made by the following seven methods of wave data input in a hypothetical case and the existing case at Bafra:

i). Method 1: Wave data input in descending order of approach angles

Wave data sets are introduced in descending order of approach angles, assuming a sign convention such that approach angle of waves, having a tendency of longshore sediment transport in right direction looking at the seaward, are set to be positive

(*Figure 5.7*). The logic behind this method is to accumulate accretion at one side and erosion at other side of structures initially, and then vice versa.

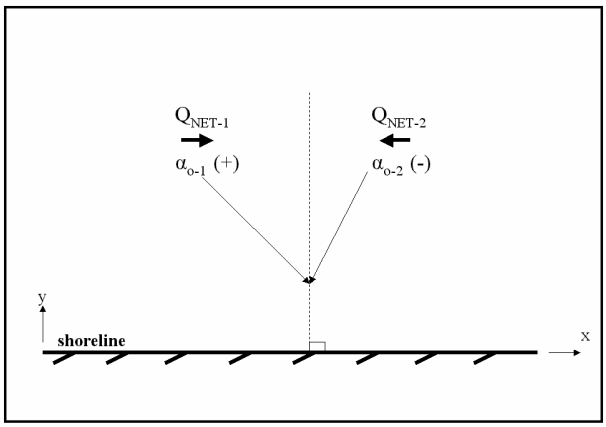

Figure 5.7 Sign convention of longshore sediment transport

ii). Method 2: Wave data input in ascending order of approach angles

This method is directly the opposite of method 1.

iii). Method 3: Wave data input in descending order of wave heights from corresponding directions

Wave data sets are put into sequence in descending order of wave heights. Such a mode of wave data input is important to observe the effect of variation of severity of storms and waves on resultant shoreline change.

iv). Method 4: Wave data input in ascending order of wave heights from corresponding directions

This method is directly the opposite of method 3.

v). Method 5: Wave data input in descending order of exceedence frequency

Wave data sets are put into sequence in descending order of exceedence frequencies. As a result of this discussion, the effect of duration of storms and waves, sequence of waves with higher/lower frequency on resultant shoreline change are observed.

vi). Method 6: Wave data input in ascending order of exceedence frequency

This method is directly the opposite of method 5.

vii). Method 7: Wave data input in a random order

The sequence of wave data sets is selected by a random number generator in the numerical model. This method is useful to achieve a *no-logic* approach to derive a statistical comparison.

In the hypothetical part of this discussion, an impermeable groin of 150 m. length is placed on an initially straight shoreline. Shoreline changes after 1 year, in the vicinity of the groin are examined by these seven methods of wave input, using annual wave data sets derived for Bafra (*Table 5.3*). Results are given below:

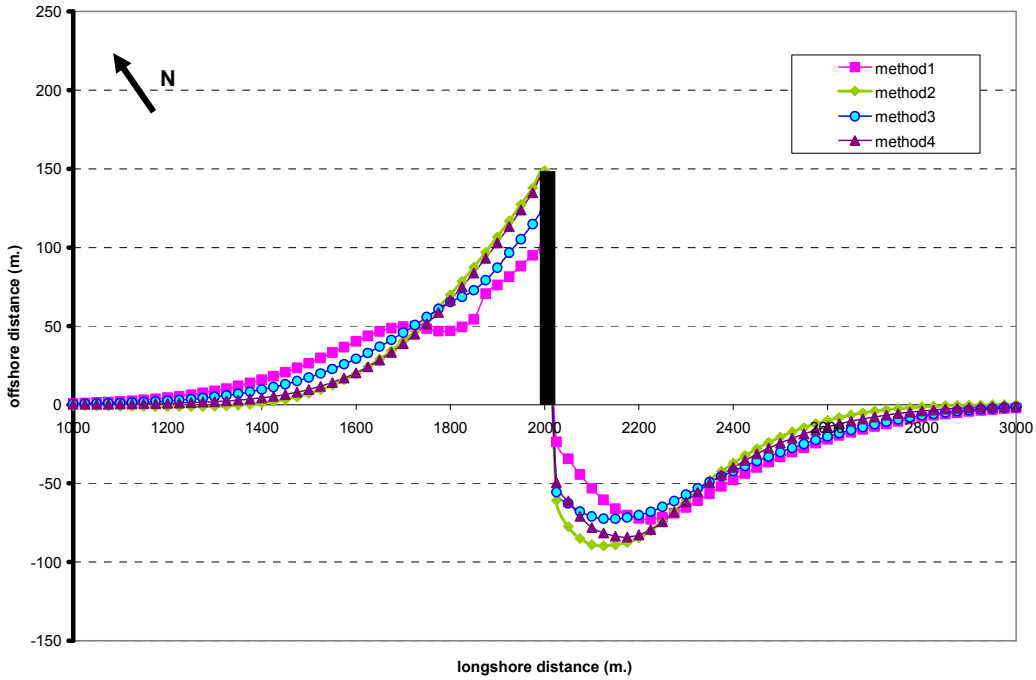

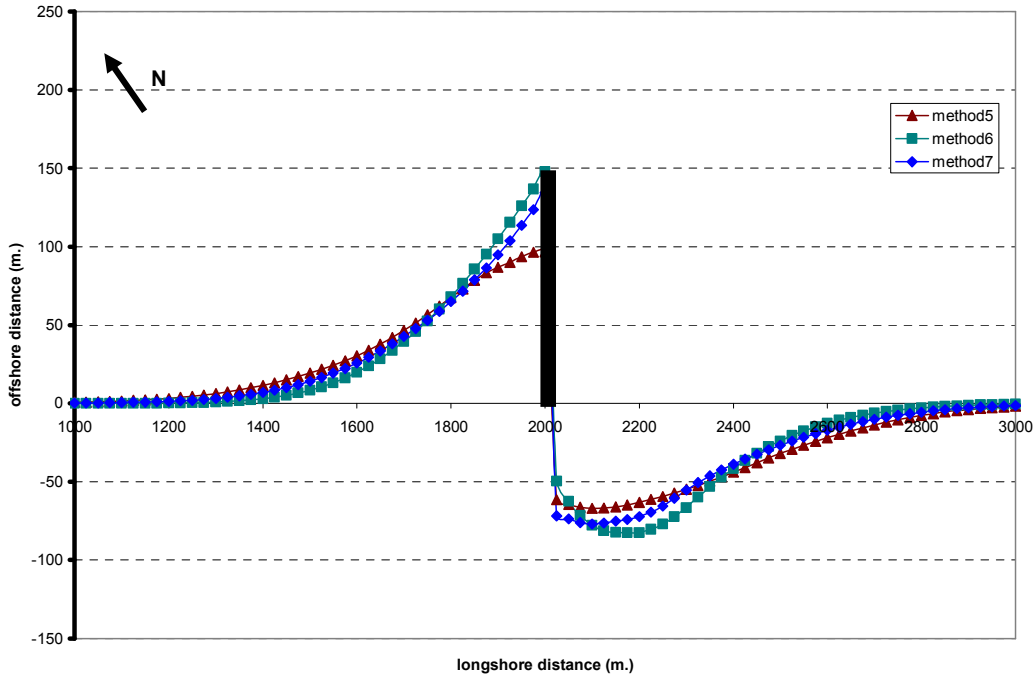

Figure 5.8 Effect of wave data input methods on shoreline change in the vicinity of a single groin

As being expected, due to the dominancy of waves from western directions, accretion occurs at western side and erosion occurs at eastern side of the groin, in the end of simulations. No significant change is observed in simulation of shoreline changes after 1 year, depending on the modes of wave data input.

5.6 Application to Bafra

In the application of the developed numerical model at Bafra, it is assumed that no source or sink exists in the region. Median grain size diameter (D_{50}) is taken as 0.23 mm. (Kökpınar et al., 2005). Besides, existing Y-shaped groins are introduced as T-shaped groins. Therefore, a similarity must be achieved to reflect the case in nature as accurate as possible. In this case study, shore parallel section of T-groin is set to reach to end of seaward *arm* of Y groins. Secondly, shore perpendicular section of T-groin is oriented similar to shore connecting section of Y-groins in region. The layout, shown in *Figure 5.9,* provides the best similarity with actual layout in *Figure 5.2*. Width of breakwater sections of T-groins is set as 150 m. and offshore length of each groin is set as 150 m.

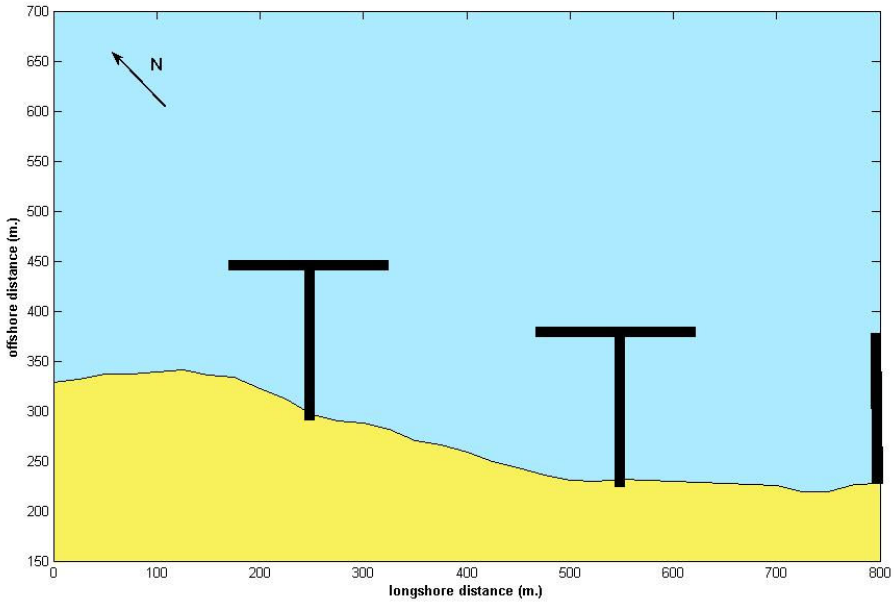

Figure 5.9 Idealized numerical boundary

The results of 4-year numerical simulations are presented in *Figure 5.10* together with the initial (April 1999) and final field measurements (January 2003).

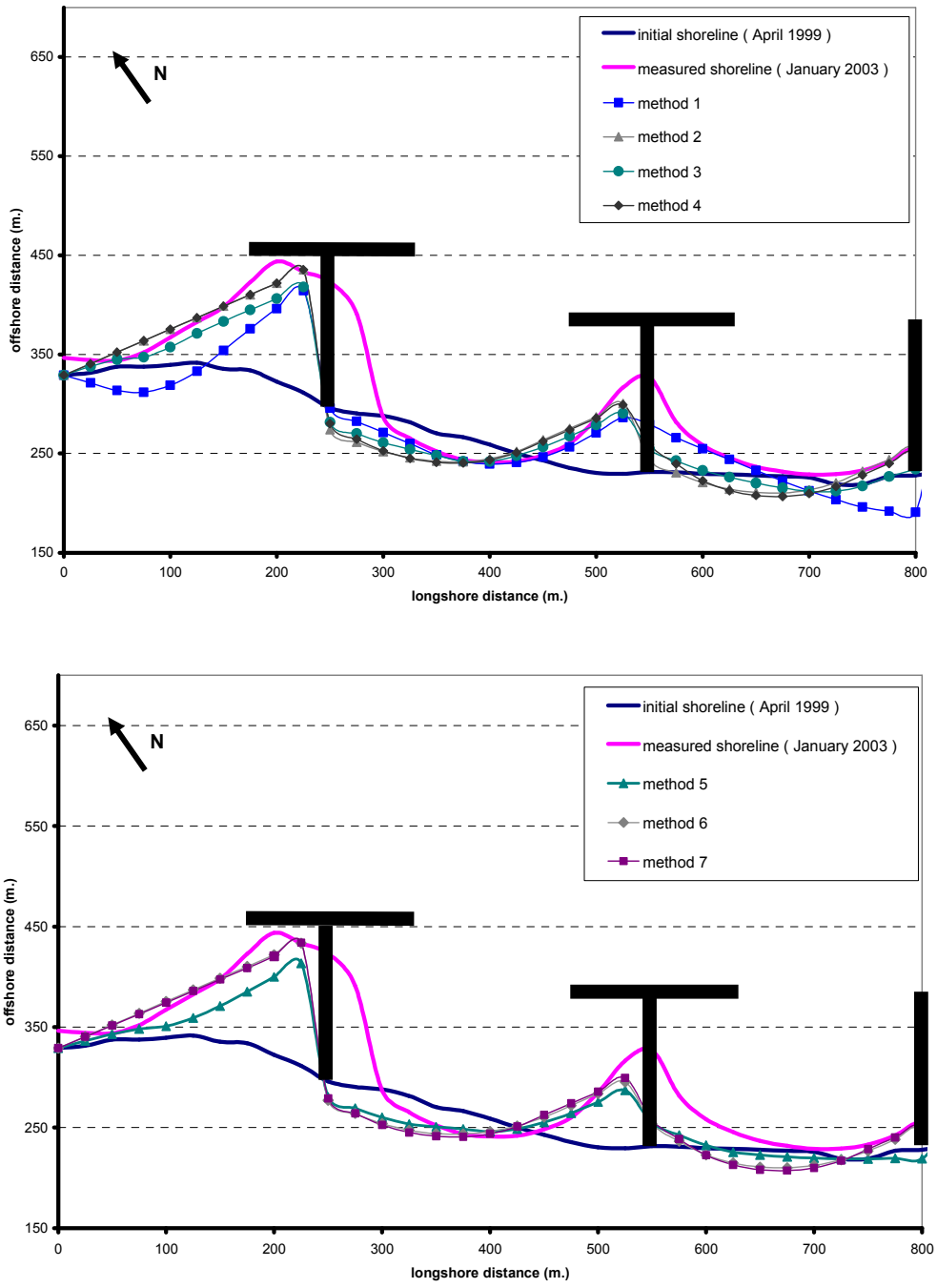

Figure 5.10 Comparison of site measurements and results of numerical simulations

As it is seen from *Figure 5.10*, resultant shoreline changes are in the same order under seven methods of wave input. In this case study, but not in general, these seven methods of wave input do not cause a significant change in model results similar to the hypothetical case with a single groin.

In overall evaluation, model results are in good agreement quantitatively with the final field measurements at left hand side of groins. However, at right hand side of Y-groins, model results are in agreement only qualitatively. These differences between model results and measurements can be attributed to the slight behaviour difference between Y-groins (field case) and T-groins (numerical model case) and measurement errors in the field, together with numerical model assumptions and use of wave data. Besides, numerical modeling of shoreline change, based on one-line theory, is challenging due to the cape-structure of the case study region. In conclusion, using annual average wave heights in the numerical model gives qualitatively comparable results with the field measurements in this case.

CHAPTER 6

CONCLUSIONS

A user-friendly numerical model, calculating shoreline changes due to wind wave induced longshore sediment transport under wide range of boundaries and constraints, is developed. Basics of one-line theory, groins, bypassing and permeability of groins, seawalls and T-groins are presented. Wave breaking and wave diffraction in the vicinity of coastal defense structures are also discussed in details. Since longshore sediment transport is taken as the major agent of shoreline changes in the developed numerical model, a limiting depth of longshore sediment transport as a function of wave breaking height is set in the model instead of depth of closure. Besides, results of the developed numerical model for beach nourishment projects are in good agreement with related analytical solution. Application of the numerical model in a case study at Bafra Delta, Black Sea, proves that model results are qualitatively consistent with the field measurements and therefore, one-line theory is successfully used in the numerical model. In this application, annual average wave data is used as wave data input, instead of actual wave time series. Input manner of wave data into the model is discussed by presenting different methods and no significant change is observed in results of the current case obtained from these methods.

Obviously, due to the fact that each coastal zone and sedimentation problem are totally different, the results of the developed numerical model needs to be compared with more field measurements at site and physical model studies and the model must be adapted to site specific conditions in order to enhance its predictions in quantity manner.

Artificial beach nourishment should be emphasized more to solve coastal sedimentation problems. Accordingly, capability of the developed numerical model, upgraded by inserting cross-shore sediment transport mechanism, to calculate shoreline changes in conjunction of nourished beaches and stabilization structures can be tested in a case study. Besides, research on submerged structures may be contributory to advancements in this profession since recent studies fail to provide distinct results in physical models, numerical models and site investigations.

In general, increasing popularity of new shore protection technologies such as geotextiles, sand tubes and gabion units must guide a designer to find the optimum solution among various methods. Whatever the taken measure is, an optimization of existing resources, detailed evaluation of desired results and monitoring after the implementation is obligatory to achieve long-term success in related projects.

REFERENCES

Artagan, S.S., (2006), "A One-Line Numerical Model for Shoreline Evolution under the Interaction of Wind Waves and Offshore Breakwaters ", M.S. Thesis, METU, Ankara (in print)

Bakker, W.T., (1969), "The Dynamics of a Coast with a Groyne System", Proceedings of 11th Coastal Engineering Conference, American Society of Civil Engineers, pg. 492-517

Baykal, C., (2006), "Numerical Modeling of Wave Diffraction in One-Dimensional Shoreline Change Model", M.S. Thesis, METU, Ankara (in print)

Beach Management Manual, (1996), Construction Industry Research and Information Association (CIRIA), London

Bijker, E.W.,(1971) , "Longshore Transport Computations", *Journal of Waterways, Harbors and Coastal Engineering Division*, ASCE, Volume 97, pg.687-701

Briand, M.H.G., and Kamphuis, J.W., (1993), "Sediment transport in the surf zone: A quasi 3-D numerical model", Coastal Engineering, Volume 20, pg.135-156

Coastal Engineering Manual (CEM), (2003), U.S. Army Corps of Engineers, Coastal Engineering Research Center, U.S. Government Printing Office

Cooper, J.A.G., Pilkey, O.H., (2004), "Alternatives to the Mathematical Modeling of Beaches" , Journal of Coastal Research, Volume 20, No.3, pg.641-644

Dabees, M.A., (2000), “Efficient Modeling of Beach Evolution”, Ph.D. Thesis, Queen’s University, Kingston, Ontario, Canada

Davison, A.T., Nicholls, R.J., Leatherman, S.P., (1992), “Beach Nourishment as a Coastal Management Tool: An Annotated Bibliography on Developments Associated with the Artificial Nourishment of Beaches”, Journal of Coastal Research, Volume 8, No.4, pg.984-1022

Dean, R.G., (1991), “Equilibrium Beach Profiles: Characteristics and Applications”, Journal of Coastal Research, Volume 7, No.1, pg. 53 – 84

Dean, R.G., Yoo, C.H., (1992), “Beach-Nourishment Performance Predictions”, Journal of Waterway, Port, Coastal and Ocean Engineering, Volume 118, No.6, pg.567-585

Ergin,A.,and Özhan, E.(1986), “15 Deniz Yöresi için Dalga Tahminleri ve Tasarım Dalgası Özelliklerinin Belirlenmesi” (in Turkish), Ocean Engineering Research Center Middle East Technical University, Ankara

Finkl, C.W., (1996), “What Might Happen to America’s Shorelines if Artificial Beach Replenishment is Curtailed: A Prognosis for Southeastern Florida and Other Sandy Regions Along Regressive Coasts”, Journal of Coastal Research, Volume 12, No.1, pg. iii-ix

Güler, I., (1997),“Investigation on Protection of Manavgat River Mouth”, Yüksel Proje International Co. Inc., Research Project Report (in Turkish)

Güler, I., Ergin, A., and Yalçıner, A.C., (1998), “The Effect of the Use of Wave Data for the Numerical Solution of Shoreline Evolution”, Journal of Coastal Research, Special Issue No.26, pg. 195-200

Goda, Y., Takayama, T., and Suzuki, Y., (1978), "Diffraction Diagrams for Directional Random Waves," Proc. 16th Int. Conf. on Coastal Engrg., ASCE, pg.628-650.

Hall, M.J., Pilkey, O.H., (1991), "Effect of Hard Stabilization on Dry Beach Width for New Jersey", Journal of Coastal Research, Volume 7, pg. 771-785

Hallermeier, R.J., (1978), "Uses for a Calculated Limit Depth to Beach Erosion", Proceedings of the 16th Coastal Engineering Conference, American Society of Civil Engineers, New York, NY, pp.1493-1512

Hanson, H. , (1987), "GENESIS: A Generalized Shoreline Change Numerical Model for Engineering Use", Ph.D. Thesis, University of Lund, Lund, Sweden

Hanson, H., Kraus, N.C., (1986a), "Seawall Boundary Condition in Numerical Models of Shoreline Evolution", Technical Report CERC-86-3, U.S. Army Engineer Waterways Experiment Station, Vicksburg, MS.

Hanson, H., Kraus, N.C., (1991), "Numerical Simulation of Shoreline Change at Lorain, Ohio", Journal of Waterway, Port, Coastal and Ocean Engineering, Volume 117, No.1, pg.1-18

Hanson, H., Kraus, N.C., (1993), "Optimization of Beach Fill Transitions", Beach Nourishment Engineering and Management Considerations-Proceedings of Coastal Zone '93, pg. 103-117 ASCE, New York

Hanson, H., Aarninkhof, S., Capobianco, M., Jimenez, J.A., Larson, M., Nicholls, R.J., Plant, N.G., Southgate, H.N., Steetzel, H.J., Stive, M.J.F., de Vriend, H.J.,

(2003), “Modelling of Coastal Evolution on Yearly to Decadal Time Scales”, Journal of Coastal Research, Volume 19, No.4, pg.790-811

Hsu, J.R.C., and Silvester,R., (1990), “Accretion Behind Single Offshore Breakwater”, *Journal of Waterway, Port, Coastal and Ocean Engineering*, ASCE,Volume 116, No.3, pg. 362 – 380

Kamphuis, J.W.,(1991), “Alongshore Sediment Transport Rate”, *Journal of Waterway, Port, Coastal and Ocean Engineering*, ASCE, Volume 117, pg.624-640

Kamphuis, J.W., (2000), “Introduction to Coastal Engineering and Management”, World Scientific

Kökpınar, M.A., Darama, Y., Güler, I., (2005), “Physical and Numerical Modeling of Shoreline Evaluation of the Kızılırmak River Mouth, Turkey”, Journal of Coastal Research, Volume 21 (in print)

Kraus, N.C., Gingerich, K.J., and Rosati, J.D., (1989), “DUCK85 Surf Zone Sand Transport Experiment” Technical Report, CERC-89-5, U.S. Army Engineer Waterways Experiment Station, Vicksburg, MS.

McCormick, M.E., (1993), “Equilibrium Shoreline Response to Breakwaters”, *Journal of Waterway, Port, Coastal and Ocean Engineering*, ASCE, Volume 119, No.6, pg.657-670

Munk, W.H., (1949), “The Solitary Wave Theory and its Application to Surf Problems”, Symposium on Gravity Waves, Circular No.521, National Bureau of Standards, Washington, D.C., pg. 376-462

Ozasa, H., and Brampton, A.H., (1980), “Models for Predicting the Shoreline Evolution of Beaches Backed by Seawalls”, Report, Hydraulics Research Station, Wallingford

Pelnard-Considere, R., (1956), “Essai de Theorie de l’Evolution des Forms de Rivage en Plage de Sable et de Galets”,4th Journees de l’Hydraulique, Les Energies de la Mer, Question III, Rapport No.1, pg. 289-298

Roelvink, J.A., and Broker, I., (1993), “Cross-shore profile models”, Coastal Engineering, Volume 21, pg. 163-191

Shore Protection Manual (SPM), (1984), U.S. Government Printing Office, Washington D.C.

Southgate, H.N., (1995), “The effects of wave chronology on medium and long term coastal morphology” , Coastal Engineering , Volume 26, pg. 251-270

Suh, K., and Dalrymple, R.A., (1987), “Offshore Breakwaters in Laboratory and Field”, Journal of Waterway, Port, Coastal and Ocean engineering, Volume 113, No.2, pg. 105 - 121

Thieler, E.R., Pilkey, O.H., Young, R.S., Bush, D.M., Chai, F., (2000), “The Use of Mathematical Models to Predict Beach Behavior for U.S. Coastal Engineering: A Critical Review”, Journal of Coastal Research, Volume 16, No.1, pg.48-70

Vrijling, J.K., Meijer, G.J., (1992), “Probabilistic Coastline Position Computations” , Coastal Engineering, Volume 17, pg.1-23

Walton, T.L., (1994), “Shoreline Solution for Tapered Beach Fill”, Journal of Waterway, Port, Coastal and Ocean Engineering, Volume 120, No.6, pg.651-655

Wang, P., Ebersole, B.A., and Smith, E.R., (2002), “Longshore Sediment Transport – Initial Results from Large Scale Sediment Transport Facility”, ERDC/CHL CHETN – II-46, U.S. Army Engineer Research and Development Center, Vicksburg, MS

APPENDIX A

FLOWCHART OF THE NUMERICAL MODEL

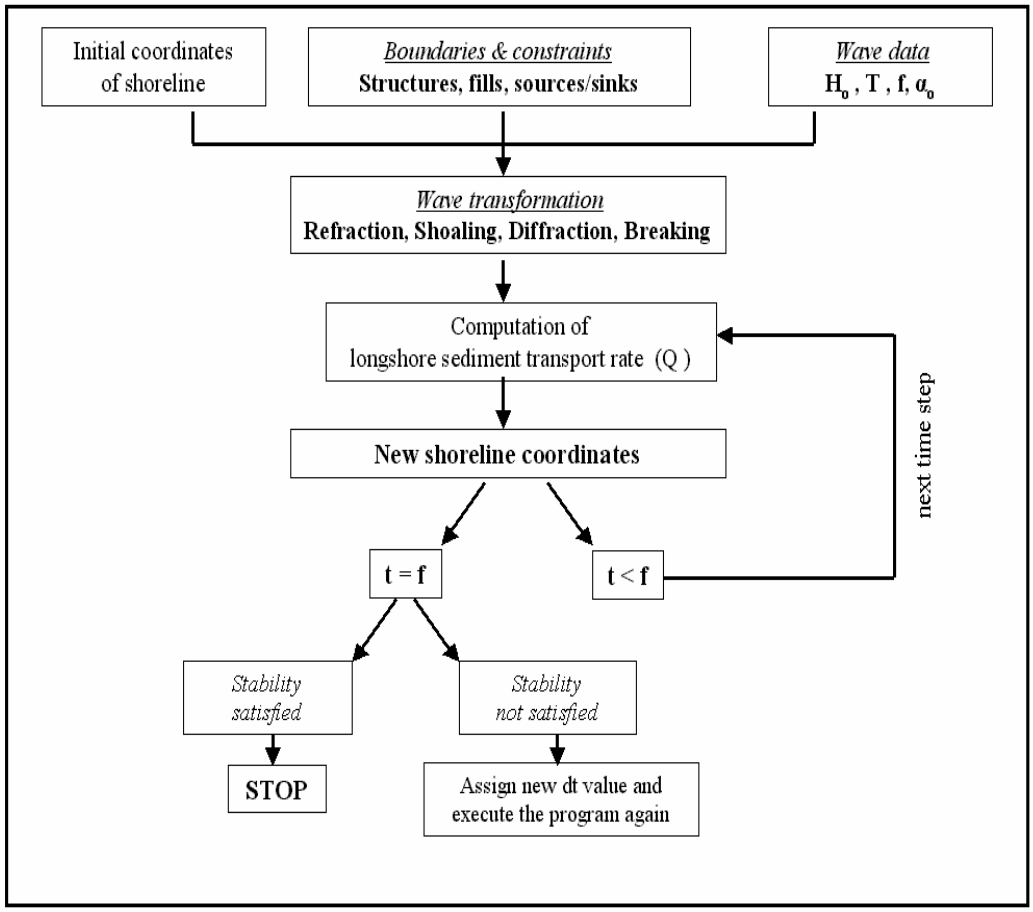

Figure A.1 Flowchart of the numerical model

APPENDIX B

EXECUTION OF THE NUMERICAL MODEL AND SAMPLE RUNS

Basic principles of execution of the developed numerical model are introduced herein. Besides, two sample runs are made in details and results are given for two different hypothetical cases.

Initial shoreline coordinates

Developed numerical model is capable of simulating wind wave induced longshore sediment transport and resulting shoreline changes both on initially straight shoreline and irregular shoreline. Therefore, initial shoreline coordinates may be entered to the model in two ways, as follows:

```
How do you enter initial shoreline coordinates?

[1]: Initially straight shoreline
[2]: Read from file
```

User must enter "1" to start a simulation on an initially straight shoreline, but still has to define the alongshore length of the modeled region in x-direction and position of shoreline in y-direction, by answering the following 2 questions:

```
Enter the length of shoreline in x-direction (in m.):
Initial shoreline coordinate in y-direction (in m.):
```

On the other hand, user can make the simulation on an irregular shoreline by entering "2" and inserting the initial shoreline coordinates (x,y) of the modeled region to a

comma-separated file, named "*kiyi_cizgisi*" . A sample shoreline coordinate input file is given below:

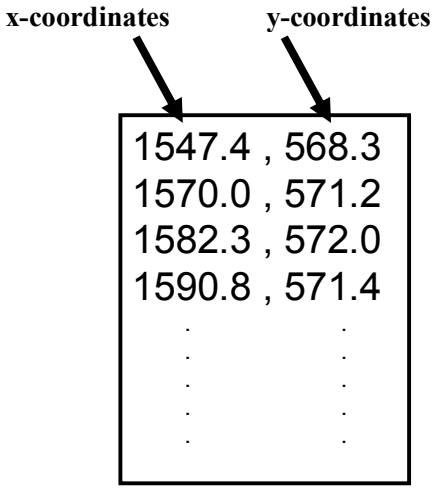

Figure B.1 Input of initial shoreline coordinates to the numerical model

In the final output of the numerical model, initial shoreline coordinates are illustrated with *red* color. Following the designation of initial shoreline coordinates, values of alongshore distance increment (dx) and time increment (dt) are defined as follows:

```
Enter the alongshore distance increment,dx, in m. :
Enter time increment, dt, in hours:
```

Regional sediment properties

Two main regional parameters, median grain size diameter (D_{50}) and beach berm height (B) are defined by user, in meters, as follows:

```
Enter the median grain size diameter (D50) in m.:
Enter beach berm height above still water level:
```

Definition of boundaries and constraints

Number of sources and sinks, beach nourishment projects and coastal defense structures are defined initially. Depending on the number of each of these boundaries and constraints, their major parameters are defined one by one. Location of each boundary and constraint is defined from the left end of the modeled region, looking at the seaward direction.

Sources and sinks

Arbitrary number of sources and sinks may be defined within the modeled region at given locations and magnitudes, where magnitude of a source is defined as positive and magnitude of a sink is defined as negative in m^2/hrs., as follows:

```
Enter the location of source/sink from left:
Enter the magnitude of source/sink:
```

In the output of the numerical model, sources/sinks are illustrated with *green* color at the related location.

Beach nourishment projects

In existence of nourishment projects, initial shoreline is shifted in offshore direction, depending on the dimensions and locations, entered by the user as follows:

```
Enter the distance of beach fill from left :
Enter the width of beach fill :
Enter the offshore distance of beach fill :
Enter taper length of beach fill :
```

It should be noted that, location and width of beach nourishment projects are defined free from tapers. Besides, current structure of the model enables the use of this module on initially straight shoreline with shoreline position, y=0.

Seawalls

Arbitrary number of seawalls can be defined by their locations, widths and onshore distances as follows :

```
Enter the distance of seawall from left :
Enter the width of seawall :
Enter the distance of seawall onshore :
```

In the final output of the numerical model, seawalls are illustrated with *black* color.

Groins

Arbitrary number of shoreline-perpendicular groins are defined by their locations, offshore lengths and permeability ratios as follows:

```
Enter the distance of groin from left :
Enter the length of groin :
Enter the permeability ratio of groin :
```

In the final output of the numerical model, impermeable groins are illustrated with *black* color, where permeable groins are illustrated with *magenta* color.

Offshore breakwaters

Arbitrary number of shoreline-parallel offshore breakwaters are defined by their locations, widths, offshore distances and permeability ratios as follows:

```
Enter the distance of offshore breakwater from left :
Enter the width of offshore breakwater :
Enter the distance of offshore breakwater offshore :
Enter the permeability ratio of offshore breakwater :
```

In the final output of the numerical model, impermeable offshore breakwaters are illustrated with *black* color, where permeable offshore breakwaters are illustrated with *magenta* color.

T-groins

Arbitrary number of impermeable groins are manually defined by defining a groin and an offshore breakwater separately. Offshore length of groin must be same with the seaward distance of breakwater from shoreline and location of groin section must be within the alongshore range of offshore breakwater. In the final output of the numerical model, T-groins are illustrated with black color.

Wave data input

Wave input file of the numerical model is a comma-separated file, named as *"dalga"*. Numerical model is applicable to wave input with either a single data set or several data sets. A data set must include deep water significant wave height in m.(H), significant wave period in sec.(T), frequency in hours (f) and deep water approach angle(α) in degrees, respectively. In the sign convention of the numerical model, approach angle of waves, having a tendency of longshore sediment transport in right direction looking at the seaward, are set to be positive. A sample wave input file with several wave data sets is given below:

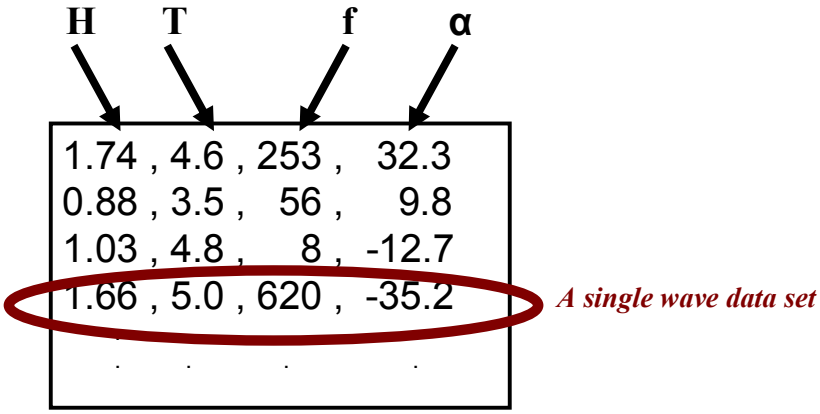

Figure B.2 Input of wave data to the numerical model

Wave data sets are taken into consideration by the numerical model in a sequence from top to bottom. Resulting shoreline, calculated from a data set, is set as the initial shoreline of next data set. User, with the intention of making a simulation with the given wave data more than once with the given order, can select the number of repetitions by answering the following question:

```
Enter the number of repetitions:
```

For instance, entering "4" means executing the program 4 times with the given wave data and the *given sequence*.

Stability check and plot

Throughout the simulations, maximum stability parameter (*Eqn.3-13*) calculated at the computations in each data set is displayed. After the end of simulation, stability is checked and if not achieved (>0.5) even for a single wave data set, user is requested to enter a smaller time increment value (dt) as follows :

```
Execute the program with a smaller dt value .
```

As long as the stability is achieved, final output of the numerical model is plotted.

Sample runs

Sample run 1

2 T-groins and 1 seawall are placed on an initially straight shoreline. Simulation is made using the single wave data set and inputs, given below:

Table B.1 Wave data input of *Sample run 1 – "dalga"* file

```
1.8,5.2,750,23
```

Initial shoreline:
[1]:Initially straight shoreline
[2]:Read from file
1
Enter the length of shoreline in m.:
2500
Initial shoreline coordinate in m.:
0
Enter the alonghsore distance increment,dx, in m. :
25
Enter time increment, dt, in hours.
2
Enter the median grain size diameter(D50) in m.:
.0006
Enter beach berm height above still water level:
3
Enter the number of sources/sinks:
0
Enter the number of seawalls:
1
Enter the distance of seawall 1 from left:

1100

Enter the width of seawall 1:

300

Enter the distance of seawall 1 onshore:

15

Enter the number of tapered beach fills:

0

Enter the number of offshore breakwaters:

2

Enter the distance of offshore breakwater 1 from left:

800

Enter the width of offshore breakwater 1:

200

Enter the distance of offshore breakwater 1 offshore:

200

Enter the permeability coefficient of offshore breakwater 1 :

0

Enter the distance of offshore breakwater 2 from left:

1500

Enter the width of offshore breakwater 2:

200

Enter the distance of offshore breakwater 2 offshore:

200

Enter the permeability coefficient of offshore breakwater 2 :

0

Enter the number of groins:

2

Enter the distance of groin 1 from left:

900

Enter the length of groin 1:

200

Enter the permeability of groin 1:

0

Enter the distance of groin 2 from left:

1600

Enter the length of groin 2:

200

Enter the permeability of groin 2:

0

Enter the number of repetitions:

1

1.9003

Execute the program with a smaller "dt" value.

Since computed stability parameter exceeds 0.5, user is requested to execute the program again with a smaller time increment value (dt) . Keeping the rest of the inputs same, time increment (dt) is decreased from 2 hours to 0.3 hours and stability is achieved with *0.3602*. Final output of the developed numerical model is given below:

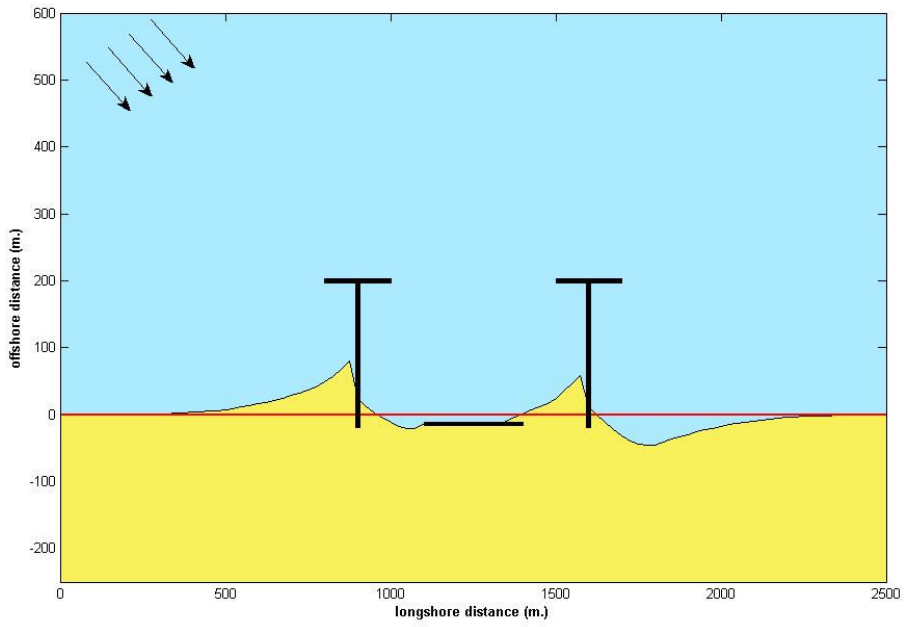

Figure B.3 Final output of *Sample run 1*

Sample run 2

6 permeable groins with varying offshore lengths are placed on an irregular shoreline. Initial shoreline coordinates are given below:

Table B.2 Initial shoreline coordinates of *Sample run 2 – "kiyi_cizgisi"* file

```
1485,636
1507,634
1529,632
1551,630
1573,628
1595,626
1617,624
1639,622
1661,620
1683,618
1705,616
1727,614
1749,612
1771,610
1793,608
1815,606
1837,604
1859,604.3
1881,604.6
1903,604.9
1925,605.2
1947,605.5
1969,605.8
1991,606.1
2013,606.4
2035,607.7
2057,609
2079,610.3
2101,611.6
2123,612.9
2145,614.2
2167,615.5
2189,616.8
2211,618.1
```

```
2233,619.4
2261,620.7
2289,622
2317,623.3
2345,624.6
2373,625.9
2401,627.2
2429,628.5
2457,629.8
2485,631.1
2513,632.4
2541,633.7
2569,635
2597,637
2625,639
2653,641
2681,643
2709,645
2737,647
2765,649
2793,651
2821,653
2849,655
2877,657
2905,659
2933,661
2961,663
2989,665
3017,667
3045,666.5
3073,666
3101,665.5
3129,665
3157,664.5
3185,664
3213,663.5
3241,663
3269,662.5
3297,662
3325,661.5
3353,661
3381,660.5
3431,660
3481,659.5
```

Simulation is made with 4 wave data sets, 2 repetitions and inputs, given below:

Table B.3 Wave data input of *Sample run 2 – "dalga"* file

```
0.8,3.8, 50,35
1.2,3.9,182,8
1.4,5  ,  9,-16
1.2,4.3,250,-53
```

Initial shoreline:

[1]:Initially straight shoreline

[2]:Read from file

2

Enter the alonghsore distance increment,dx, in m. :

25

Enter time increment, dt, in hours.

.5

Enter the median grain size diameter (D50) in m.:

.0008

Enter beach berm height above still water level:

2

Enter the number of sources/sinks:

0

Enter the number of seawalls:

0

Enter the number of tapered beach fills:

0

Enter the number of offshore breakwaters:

0

Enter the number of groins:

6

Enter the distance of groin 1 from left:

350

Enter the length of groin 1:

150

Enter the permeability of groin 1:

.3

Enter the distance of groin 2 from left:

650

Enter the length of groin 2:

130

Enter the permeability of groin 2:

.3

Enter the distance of groin 3 from left:

950

Enter the length of groin 3:

120

Enter the permeability of groin 3:

.3

Enter the distance of groin 4 from left:

1200

Enter the length of groin 4:

120

Enter the permeability of groin 4:

.3

Enter the distance of groin 5 from left:

1450

Enter the length of groin 5:

100

Enter the permeability of groin 5:

.3

Enter the distance of groin 6 from left:

1650

Enter the length of groin 6:

70

Enter the permeability of groin 6:

.3

Enter the number of repetitions:

2

0.0162

0.2361

0.1044

0.0463

0.0154

0.2360

0.1300

0.0489

With the inputs given above, final output of the developed numerical model is as follows:

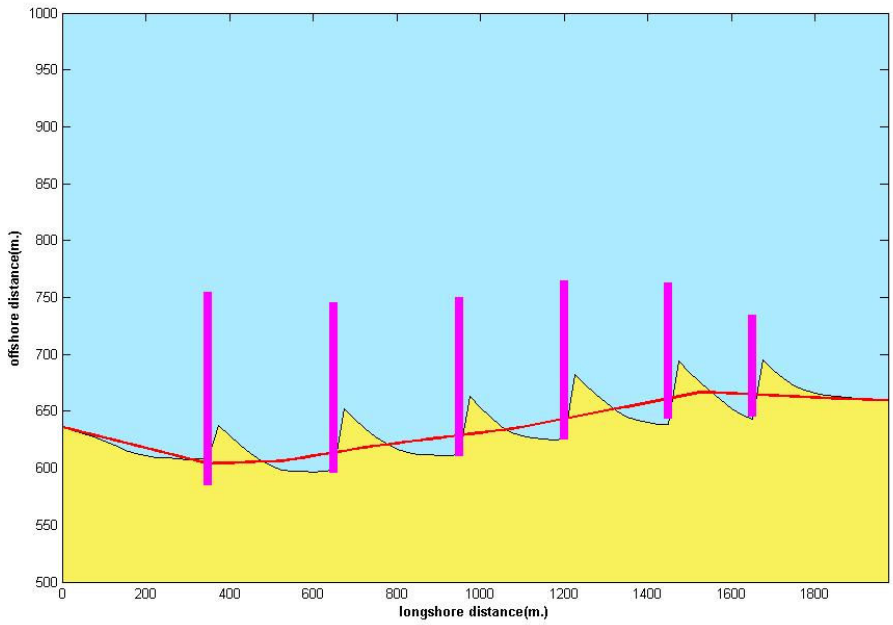

Figure B.4 Final output of *Sample run 2*